UNITED STATES DEPARTMENT OF THE INTERIOR

GEOLOGICAL SURVEY

SUPPLEMENTAL RESOURCE REPORT FOR OCS LEASE SALE #83 NAVARIN BASIN, ALASKA

by

Michael S. Marlow[1]; Alan K. Cooper[1]; Paul R. Carlson[1]; Herman A. Karl[1]; and Brian D. Edwards[1].

Open-File Report 83-707

This report is preliminary and has not been reviewed for conformity with U.S. Geological Survey editorial standards and stratigraphic nomenclature.

1. U.S. Geological Survey
345 Middlefield Road
Menlo Park, California 94025

1983

PREFACE

The following report is a supplement to the original resource report by Marlow et al. (1981), which should be consulted for a more thorough review of Navarin basin. The first part of this supplement is taken from a paper by Marlow et al. (1983). The second part of the supplement is abstracted from a report by Cooper and Marlow (1983). Part three is from Carlson and others (1983). These reports discuss the partial results of field work conducted in 1980 and 1982 by the Geological Survey. No revision or update is included for the petroleum geology section, and there is no section on hard minerals geology.

TABLE OF CONTENTS

PART I - GEOLOGIC FRAMEWORK

ABSTRACT

The Gulf of Anadyr is underlain by two major sedimentary basins, Kresta basin and East Anadyr trough, that trend east to southeast and contain, in places, more than 9 km of fill. The basins are flanked to the east and north by the Okhotsk-Chukotsk volcanic belt, a broad bedrock high composed of plutonic and volcanic rocks that extends from eastern Siberia along the inner Bering Sea shelf at least to St. Matthew Island. The East Anadyr trough extends onshore and connects with the larger Anadyr basin, which underlies the lowlands between the Koryak Range and Okhotsk-Chukotsk volcanic belt of eastern Siberia.

New seismic-reflection and refraction data reveal that Anadyr basin is separated from Navarin basin by Anadyr ridge, a southeast-northwest-trending bedrock high that is characterized by high-amplitude, short-wavelength magnetic anomalies. Anadyr ridge may be an offshore extension of the melange belt underlying the Koryak Range. Sonobuoy refraction data indicate that the velocity profile of strata in East Anadyr trough is similar to that in Navarin basin. Structurally, however, the basins are different: Navarin basin is complex and contains both compressional and extensional elements, whereas Anadyr basin is a simple, broad crustal sag semicircular in outline. Correlation of our reflection data from the offshore part of the Anadyr basin (including the East Anadyr trough and Kresta basin) with

drilling data onshore allow us to differentiate three distinct sequences in the offshore portion of the basin. These sequences are separated by two strong reflectors, a and b, and are tentatively identified with increasing depth as boundaries separating the Paleogene, and Mesozoic respectively.

INTRODUCTION

Proposed leasing of the outer continental shelf (OCS) in the Bering Sea for hydrocarbon exploration has led to increased interest in a number of large basins beneath the shelf, west of Alaska. One of these basins, Navarin, underlies the shelf west of St. Matthew Island, near the 1867 U.S.-U.S.S.R. Convention Line (Fig. 1). North of Navarin basin, the Bering shelf is underlain by Anadyr basin, which extends onshore and underlies parts of eastern Siberia (Verba et al., 1971; Kummer and Creager, 1971; Meyerhoff, 1972; Burlin et al., 1974; Verba and Yermakov, 1976). Anadyr basin encompasses approximately 35,000 sq km onshore and nearly 40,000 sq km offshore. Since 1959, the Soviet Union has drilled 30 exploratory and stratigraphic-test wells in the onshore portion of Anadyr basin (McLean, 1979).

Gas shows in Miocene sandstone and oil and gas shows in Eocene and Oligocene strata occurred in wells drilled onshore in Anadyr basin (Agapitov et al., 1970, 1973; Meyerhoff, 1972; Burlin et al., 1975), indicating the existence of possible source beds onshore; however, to date no wells have been drilled in the offshore portion of Anadyr basin.

In 1980 the U.S. Geological Survey collected geophysical data along 1,800 km (980 nautical miles) of trackline in the Gulf of Anadyr and over northern Navarin basin to evaluate the offshore extent of both basins (Fig. 2). Data collected include 24-channel seismic-reflection profiles using a tuned five-airgun array as the sound source (total capacity, 21.7P), high- resolution seismic-reflection profiles, and bathymetry, gravity, and magnetic data. These data are compared with published structural and stratigraphic data from the onshore portion of Anadyr basin in order to interpret the structure and stratigraphy of the offshore portion of Anadyr basin and nearby Navarin basin. Although our data show that Anadyr and Navarin basins are separate, structurally distinct features, the similarity in the velocity profile of each basin's fill suggests that they had similar depositional histories. Thus, relating the geologic history of Anadyr basin onshore to that of Navarin basin and the offshore portion of Anadyr basin is important in estimating whether either basin contains suitable source beds for hydrocarbons.

In this report we outline the geologic setting of Anadyr basin including East Anadyr trough and present portions of our geophysical data collected in the Gulf of Anadyr and northern Navarin basin. We further speculate on the evolution of the northern Bering Sea shelf and its relation to ancient plate boundaries in the north Pacific.

GEOLOGIC SETTING

The region surrounding Anadyr and Navarin basins can be divided into distinct lithologic belts mapped in eastern Siberia and in part on St. Lawrence Island, belts which presumably extend offshore beneath the northern Bering Sea (Figs. 3, 4).

Pre-Cretaceous Rocks

The oldest and northernmost belt consists of pre-Cretaceous miogeoclinal rocks, which extend from Chukotsk Peninsula southward as far as St. Lawrence Island and then turn northward across the Seward Peninsula and into the Brooks Range of Alaska (Krasnyy, 1965; Churkin, 1970; Patton and Tailleur, 1977; Churkin and Trexler, 1980; Patton and Csejtey, 1979). Paleozoic shelf carbonate rocks similar to those present in the Brooks Range are found in the eastern and northern parts of the Chukotsk Peninsula (Churkin, 1973). The pre-Cretaceous miogeoclinal rocks are part of an east-west belt that is thought to have been deflected to the south by east-west compression and crustal shortening during Late Cretaceous or early Paleogene time (Patton and Tailleur, 1977).

Okhotsk-Chukotsk Volcanic Belt

The Okhotsk-Chukotsk volcanic belt flanks the miogeoclinal belt on the south. This magmatic arc underlies the northern portion of Anadyr basin and is the eastern boundary of Navarin basin. This arcuate complex consists mainly of calc-alkaline volcanic and plutonic rocks of Cretaceous and early Tertiary age and can be traced from the Chukotsk Peninsula southeast through St. Lawrence Island across the Bering Sea shelf to St. Matthew Island (Fig. 4; Verba et al., 1971, Patton et al., 1974, 1976; Scholl et al., 1975; Marlow et al., 1976). However, coeval igneous rocks are also found in a broad belt in western Alaska, which can be traced for 800 km from the lower Kuskokwim River valley to the Arctic Circle (Patton et al., 1976, Fig. 4). The Okhotsk- Chukotsk volcanic belt is probably the product of convergence and subduction of oceanic lithosphere (Kula plate?) beneath the Mesozoic Beringian continental margin and eastern Siberia (Scholl et al., 1975; Marlow et al., 1976).

Forearc Sedimentary Basins

Anadyr and Navarin are forearc basins south and west of the Okhotsk-Chukotsk volcanic belt that contain thick sedimentary sequences (Fig. 1). Onshore, Anadyr basin underlies the lowlands that are flanked on the north, west and south by the Koryak Range. Offshore, the East Anadyr trough and Navarin basin underlie the virtually flat Bering Sea shelf and contain thick sedimentary sequences, which in places exceed 12 km.

Koryak Range

The eastern Koryak Range flanks the south side of Anadyr basin

(Fig. 1) and is underlain by structurally juxtaposed blocks of different age and lithology that make up the Koryak foldbelt. McLean (1979) compares the complex structural fabric of the Koryak Range to the Franciscan assemblage in California. Sequences common to both areas include chert, siliceous shale, siltstone, fine-grained graywacke, spilite, tuff, pillow basalt, blueschist, and ultramafic rocks.

Large slabs that include olistostrome and melange sequences occur within the Koryak Range and are separated by northward- dipping thrust faults (Aleksandrov et al., 1976). Blocks in the olistostrome and serpentinite melange include shallow-water Devonian, Carboniferous, and Lower and Upper Permian limestone. The Paleozoic blocks in the Koryak Range are allochthonous units that were tectonically derived from the south, in the vicinity of the present-day Bering Sea by the late Mesozoic or the earliest Tertiary (Aleksandrov et al., 1976).

The Koryak Range, like the ranges of southern Alaska, may have formed from the amalgamation of northward-moving terranes that accreted against nuclear Siberia (Siberian platform) before the formation of the Bering Sea at the end of Mesozoic or in the earliest Cenozoic (Scholl et al., 1975). Anadyr basin presumably began to form during the Cretaceous as a forearc basin situated between the Chukotsk magmatic arc to the north and east and the Koryak melange belt to the south.

OFFSHORE DATA FROM ANADYR AND NAVARIN BASINS

Seismic Refraction Data

Thirty-five sonobuoy refraction lines were shot in the vicinity of Anadyr and Navarin basins in 1976, 1977, and 1980 (Fig. 5). The results from those stations are listed in Table 2 and shown on Figures 6 and 7. The sonobuoy refraction stations are grouped by structural areas, as identified from seismic- reflection profiles.

To compare the acoustic velocity value of strata in Anadyr basin with those of strata in Navarin basin, refraction velocities were plotted as a function of depth for all sonobuoys in each basin, and then the points for each plot were fit by least squares (Fig. 7). Except for the deepest refractors, each data set is highly linear. The resulting best-fit lines for Anadyr and Navarin basins are similar. The similarity of the velocity-depth profiles suggests that acoustically the depths of burial of and ages of strata in Anadyr and Navarin basins are similar.

We have plotted on Figure 8 the linear regression-lines for velocity-depth data from Navarin and offshore Anadyr basins from Figure 7 with the onshore refraction data from Dolzhanskiy et al. (1966). For any given depth, the refraction velocities from onshore Anadyr basin are higher than the velocities from offshore Anadyr and Navarin basins. This disagreement may indicate that the onshore section of Anadyr basin is more consolidated than the offshore strata, perhaps as a result of greater compaction and subsequent uplift of the onshore basin fill relative to the undeformed offshore section. seismic-reflection section.

Seismic-refraction and reflection data from the offshore Anadyr basin reveal that two major reflecting and refracting horizons are present. These horizons, herein informally referred to as a and b, are shown schematically in the profiles, and the refraction velocities associated with each horizon are listed in Table 3 (see Marlow et al., 1983). The refraction velocities along horizons a and b range from 3590 to 3950 m/s and from 4340 to 4780 m/s, respectively (Table 1).

Seismic-Reflection Data

Line 9

Line 9 is located south of the Gulf of Anadyr in the Navarin basin province (Figs. 2 and 14; Marlow, 1979). The line crosses the province in an area where the basin fill is extremely thick. Reflectors can be traced to depths below 6 seconds (12 km; Fig. 14), and nearby sonobuoy 46-30 recorded crustal refractions in the basin from layers as deep as 13 km (Fig. 2, Table 2). The central basin fill is arched into a diapirlike structure that is also characterized by a local gravity high superimposed on a regional basin gravity low (Fig. 14). Bright spots or "wipe-out" zones occur near the seafloor in the arched area, suggesting the presence of gas in the shallow sedimentary section over the arch.

Along the northern portion of line 9, strata are folded and tilted and dip to the southwest. The folds are cut by a major unconformity along reflector b. A gravity high of about 25 milligals also reflects the rising bedrock surface. We believe that the folding and truncation of the fill in northern Navarin basin section maybe of late Miocene and Pliocene age because the folding is probably related to deformation and uplift of the nearby Koryak Range (Marlow, 1979). However, we have no age control for the basin as it has not been drilled.

Structure Contours

Structure contours on top of the basement horizon (drawn from measurements from the seismic-reflection records) reveal that the Gulf of Anadyr is underlain by a series of northwest- trending structural ridges and basins (Fig. 15). From south to north the gulf contains three filled basins: Oomyousik, East Anadyr trough and Kresta basin. The deepest basin, Oomyousik, contains more than 12 km of sediment; we have only one line across the basin so its orientation is unknown (contours shown on Fig. 15 for Oomyousik basin are drawn perpendicular to the ship's track). East Anadyr trough trends northwest-southeast to about 177W, where the basin turns to trend north-south. The basin fill is thickest in the southern portion of the trough, where the section is over 9 km thick (Fig. 15). Kresta basin contains more than 5 km strata.

Three structural highs underlie the Gulf of Anadyr and flank the East Anadyr trough. To the north, the Anaut uplift separates Kresta and Anadyr basin (Fig. 15). This high is apparently associated with the onshore Zolotoy uplift, which in turn is underlain by igneous rocks of Late Cretaceous age (McLean, 1979).

The east edge of the East Anadyr trough is flanked by a basement high trending north-south (Fig. 15). This high extends onshore to the north (Verba et al., 1971) and is part of the Okhotsk-Chukotsk calc-alkalic volcanic belt of late Mesozoic age. The Okhotsk-Chukotsk belt trends to the southeast toward Nunivak arch, another basement high that flanks Navarin basin and is exposed on St. Matthew Island (Fig. 1; Scholl et al., 1975; Marlow et al., 1976).

The southwest side of the East Anadyr trough is flanked by Anadyr ridge, which trends northwest-southeast (Fig. 15). The ridge strikes toward the Koryak Range, which is underlain by numerous ophiolitic slabs that contain volcanic remnants of oceanic crust as well as ultrabasic bodies (Aleksandrov, 1973). Therefore, Anadyr ridge may be an offshore extension of the Koryak Range and may be composed of the same melange units. The southeastern continuation of Anadyr ridge isolates the southern portion of the eastern Anadyr trough from the northern Navarin basin.

GEOLOGIC HISTORY

Reconstructions of plate motions for the North Pacific suggest that during the Mesozoic, prior to formation of the Aleutian arc, the Bering Sea continental margin (Beringia) was a zone of either oblique underthrusting or transform motion between the North American and Kula(?) plates (Scholl and Buffington, 1970; Moore, 1972, 1974; Scholl et al., 1975; Marlow et al., 1976; Cooper et al., 1976; Patton et al., 1974, 1976). Plate motion during the Mesozoic probably consisted of direct convergence between the Kula plate and nuclear Siberia. Subduction of the Kula plate beneath Siberia presumably resulted in the formation in part of the Okhotsk-Chukotsk volcanic arc (Scholl et al., 1975; Patton et al., 1976; Marlow et al., 1976). South of the Okhotsk-Chukotsk volcanic belt, the melange and olistostrome units now exposed as discrete tectonic terranes in the Koryak Range (Aleksandrov et al., 1976) were formed by obduction of fragments scraped off the Kula plate (Fig. 1; Scholl et al., 1975).

Uplift of the Okhotsk-Chukotsk volcanic belt as it formed and uplift of the Koryak melange belt during the middle Cretaceous presumably resulted in relative crustal downwarping of the intervening area and the initial formation of the forearc Anadyr basin. The bedrock sequence in the offshore portion of Anadyr basin, as deduced from seismic-reflection data and extrapolation of onshore geology consists of strongly folded and broken tectonic blocks of Upper Jurassic and Lower Cretaceous rocks (Agapitov et al., 1973; Burlin et al., 1974; McLean, 1979). This basement complex probably forms the lower reflecting sequence below the b horizon) in our seismic-reflection profiles and is characterized by refraction velocities of 5 km/sec or greater (Figs. 6, 9, 11, 12, 13,). Our offshore data suggest that the pre-Cretaceous sequence below Anadyr basin is broadly deformed into a broadly semicircular sag that trends to the southeast beneath the Gulf of Anadyr.

McLean (1979) compares Anadyr basin and the flanking Okhotsk-Chukotsk volcanic arc to the Great Valley sequence in central California and its flanking Sierra Nevadan plutonic belt. The Great Valley sequence, which fills a forearc basin, is flanked on its seaward side by the Franciscan rocks of coastal California. This sequence of tectonic elements is similar to the sequence near Anadyr basin inasmuch as the Anadyr basin is bounded seaward by the Koryak assemblage of eastern Siberia. In summary, Anadyr basin was a forearc basin, semicircular in outline, that formed during the Mesozoic with the concurrent development of the Okhotsk-Chukotsk volcanic arc and the Koryak melange belt. Anadyr basin has apparently continued to be filled throughout the Cenozoic even though the basin has been isolated from plate motions in the north Pacific during most of the Cenozoic.

In contrast, Navarin basin south of Anadyr is a more complex crustal feature. The northern portion of the basin is a wide crustal downwarp, which in places has subsided at least 13 km (Fig. 14; Table 2). The southern portion of the basin is a series of elongate grabens that parallel the Beringian margin (Marlow, 1979; Marlow et al., 1981).

Navarin basin, like Anadyr basin, is flanked on its landward side by the Okhotsk-Chukotsk volcanic arc (Fig. 16). However, dredge data from the continental slope seaward of Navarin basin suggest that the basin is not flanked by a southern extension of the Koryak melange belt. Rather, the continental slope of the Beringian margin is underlain by shallow-water, Mesozoic rocks that are a continuation of a belt of similar rocks exposed along the Alaska Peninsula (Marlow et al., 1979, 1982). Geologic evidence is lacking for the existence of Mesozoic accretionary melange sequences along the Beringian margin, sequences which might be expected from oblique underthrusting of the Kula plate. However, the Beringian margin may have been a transform boundary during the Mesozoic, subject to strike-slip motion rather than convergence and accretion. Such motion could have resulted in wrench faulting and extensional deformation of the margin, producing the early depocenters of Navarin basin along a margin analogous to the Cenozoic continental borderland of southern California. Presumably, blocks of scraped-off and accreted material that may have originally been attached to the Beringian margin during the Mesozoic were rafted into the Koryak Range of eastern Siberia by transform motion along the margin.

Formation of the Aleutian arc and isolation of a trapped portion of the Kula (?) plate presumably isolated the Bering Sea from plate motions by the latest Mesozoic and the earliest Tertiary (Scholl and Buffington, 1970; Moore, 1972, 1974; Scholl et al., 1975; Cooper et al., 1976; Marlow et al., 1976; Patton et al., 1976). Our seismic-reflection data suggest that the northwestern portion of the Gulf of

Anadyr, in the vicinity of the Anaut uplift, was subjected to late Cenozoic deformation and uplift (Figs. 2, 9 and 10). Seismic-reflection profiles east of Cape Navarin in the Gulf of Anadyr also show evidence of late Cenozoic deformation of strata beneath the Gulf of Anadyr (Figs. 2, 12, and 13). In contrast, the same profiles show onlap of undeformed stratified sequences across the Okhotsk-Chukotsk volcanic belt.

REFERENCES CITED

Agapitov, D. I., V. V. Ivanov, and V. G. Krainov, 1973, New data on the geology and prospects in petroleum/gas-bearing Anadyr basin; Akad. Nauk SSR North-East Group Inst. of Interior Center Trans., v. 49, p. 23-29 (in Russian).

Agapitov, D. I., Yu. K. Burlin, I. E. Drabkin, V. V. Ivanov, E. N. Kastilev, and Ya. G. Moskuin, 1970, Results of the geological exploration for oil and gas in the Anadyr basin and goals in connection with future explanations: Geologiya Nefti i Gaza, no. 8, p. 22-25 (in Russian).

Aleksandrov, A. A., 1973, Serpentinite Melange in the upper course of the Chirynay River, Koryak Highlands: Geotectonics, v. 4, p. 232-236.

Aleksandrov, A. A., N. A. Bogdanov, S. G. Byalobzheskiy, M. S. Markov, S. M. Til'man, V. Ye. Khain, and A. D. Chekhov, 1976, New data on the tectonics of the Koryak highlands: Geotectonics, v. 9, no. 5, p. 292-299.

Burlin, Yu. K., A. YA. Arkinpov, N. B. Vassoyevich, A. A. Trofimuk, and A. V Ovcharenko, 1975, Sedimentary basins of the far east and the northeast of the U.S.S.R. and their possible oil and gas content: 9th World Petroleum Cong., Tokyo, Proc., v. 3, p. 39-50.

Burlin, Yu. K., V. V. Dontsov, and T. N. Pastukhova, 1974, Further direction of oil and gas exploraton in northeastern U.S.S.R.: Geologiya Nefti i Gaza, no. 5, p. 17-22 (in Russian); 1975, Summary in Petroleum Geology, v. 12, no. 5, p. 222-223.

Carlson, P. R., H. A. Karl, and B. D. Edwards, 1983, Puzzling mass movement Features in the head of Navarinsky Canyon, Bering Sea: Geo-Marine Letters, in press.

Churkin, M., Jr., 1970, Foldbelts of Alaska and Siberia and drift between North America and Asia: In: W. L. Adkison and M. M. Brosge, eds., Proceedings of the geological seminar on the North Slope of Alaska, Am. Assoc. Pet. Geol. Pac. Sec., p. G1-G17.

Churkin, M., Jr., 1973, Paleozoic and Precambrian rocks of Alaska and their role in its structural evolution. U.S. Geological Survey Prof. Paper 740, 64 p.

Churkin, M., Jr., and J. H. Trexler, Jr., 1980, Circum-Arctic plate accretion-isolating part of a Pacific plate to form the nucleus of the Arctic Basin: Earth and Planetary Sci. Letters, v. 48, p. 356-362.

Cooper, A. K., D. W. Scholl, and M. S. Marlow, 1976, Plate tectonic model for the evolution of the Bering Sea basin: Geol. Soc. America Bull.; v. 87, p. 1119-1126.

Cooper, A. K., and M. S. Marlow, 1983, Preliminary results of geophysical and geological studies of the Bering Sea shelf during 1982: U. S. Geological Survey Open-File Report 83-322, 8p.

Dolzhanskiy, B. G., V. V. Ivanov, V. V. Dontsov, Yu. K. Burlin, and G. I. Roshchin, 1966, New data on the subsurface structure of the central part of the Anadyr basin: Geologiya Nefti i Gaza, no. 10, p. 15-20 (in Russian).

Krasnyy, L. T., 1965, Geologicheskaya karta severo-zapadnoi chasti Tikhookeanskogo podnizhnogo poyasa (Geologic map of the northwestern part of the Pacific mobile belt): Moscow, Ministry Geol. SSSR, scale 1:1,500,000.

Kummer, J. T., and J. S. Creager, 1971, Marine geology and Cenozoic history of the Gulf of Anadyr: Marine Geol., v. 10, p. 257-280.

Marlow, M. S., 1979, Hydrocarbon prospects in Navarin basin province, northwest Bering Sea shelf: Oil and Gas Journal, Oct. 29, p. 190-196.

Marlow, M. S., A. K. Cooper, D. W. Scholl, and H. McLean, 1982, Ancient plate boundaries in the Bering Sea region: In: J. H. Leggett (ed.), Trench-fore-arc geology: sedimentation and tectonics on modern and ancient active plate margins, p. 201-212.

Marlow, M. S., D. W. Scholl, A. K. Cooper, and E. C. Buffington, 1976, Structure and evolution of Bering Sea shelf south of St. Lawrence Island: AAPG Bull., v. 60, p. 161-183.

Marlow, M. S., D. W. Scholl, A. K. Cooper, and D. L. Jones, 1979, Mesozoic rocks from the Bering Sea: The Alaska-Siberia connection: Geol. Soc. America Abstracts with Programs, v. 11, no. 3, p. 90.

Marlow, M. S., P. Carlson, A. K. Cooper, H. Karl, H. McLean, R. McMullin, and M. B. Lynch, 1981, Resource report for proposed OCS sale no. 83, Navarin basin, Alaska: U.S. Geol.

Survey Open-File Rept. 81-252, 83 p.

McLean, H., 1979, Review of petroleum geology of Anadyr and Khatyrka basins, U.S.S.R.: AAPG Bull., v. 63, p. 1467-1477.

Meyerhoff, A. A., 1972, Russians look hard at the Anadyr basin: Oil and Gas Jour., Oct. 23, p. 128-129; Oct. 30, p. 84-89.

Moore, J. C., 1972, Uplifted trench sediments-southwestern Alaska-Bering shelf edge: Science, v. 175, p. 1103-1105.

Moore, J. C., 1974, The ancient continental margin of Alaska, In: C. A. Burk and C. L. Drake, eds., The geology of continental margins: New York, Springer-Verlag Inc., p. 811-816.

Patton, W. W., Jr., and I. L. Tailleur, 1977, Evidence in the Bering Strait region for differential movement between North America and Eurasia: Geol. Soc. America Bull., v. 88, p. 1298-1304.

-----, M. A. Lanphere, T. P. Miller, and R. A. Scott, 1974, Age and tectonic significance of volcanic rocks on St. Matthew Island, Bering Sea, Alaska (abs.): Geol. Soc. America Abs. with Programs, v. 6, p. 9905-9906.

-----, 1976, Age and tectonic significance of volcanic rocks on St. Matthew Island, Bering Sea, Alaska: U.S. Geol. Survey Jour. Research, v. 4, p. 67-73.

Patton, W. W., Jr., and B. Csejtey, Jr., 1979, Geologic map of St. Lawrence Island, Alaska: U.S. Geological Survey Misc. Investigations Map I-1203, scale 1:250,000.

Scholl, D. W., and E. C. Buffington, 1970, Structural evolution of Bering continental margin (abs.): Cretaceous to Holocene: AAPG Bull., v. 54, p. 2503.

Scholl, D. W., E. C. Buffington, and M. S. Marlow, 1975, Plate tectonics and the structural evolution of the Aleutian-Bering Sea region: In: Forbes, R. B., ed., Contributions to the geology of the Bering Sea basin and adjacent regions: Geol. Soc. America Spec. Paper 151, p. 1-32.

Verba, M. L., and B. V. Yermakov, 1976, Tectonic zoning of the northwestern part of the Bering Sea shelf and adjoining coastal regions: Geotectonics, v. 10, p. 142-174.

Verba, M. L., G. I. Gaponenko, S. S. Ivanov, A. N. Orlov, V. I. Timofeyev, and Yu. F. Chernenkov, 1971, Deep structure of the northwestern part of the Bering Sea and the prospects of finding oil and gas: Geofiz. Metody Razv. Arkt., no. 6, p. 70-74 (in Russian).

Yanshin, A. L., ed., 1966, Tectonic map of Eurasia: Moscow Geol. Inst. Acad. Sci. USSR, (in Russian), scale 1:5,000,000.

FIGURE CAPTIONS

Figure 1. Location of Koryak Range, Chukotsk Peninsula, Gulf of Anadyr, and Khatyrka, Anadyr, and Navarin basins.

Figure 2. Trackline chart of multichannel seismic-reflection surveys across southern Bering Sea shelf. Heavy (numbered) tracklines are profiles shown in Figures 9 - 13. Albers equal-area projection.

Figure 3. Generalized geologic map of eastern Siberia modified from Yanshin (1966).

Figure 4. Tectonic and geologic elements of eastern Siberia and the adjacent Bering Sea.

Figure 5. Offshore locations of sonobuoy refraction stations grouped by structural subprovince: K, Kresta basin; Ch, Okhotsk-Chukotsk volcanic belt; A, East Anadyr trough; AR, Anadyr ridge; N, Navarin basin. Circle with four tick marks is a dry well; circle with six tick marks is a gas well. Albers equal-area projection.

Figure 6. Sonobuoy refraction stations from the Gulf of Anadyr and Navarin basin, northern Bering Sea. Locations of stations are shown on Figure 5. Listing of results is shown in Table 2. Velocities are shown in km/sec for each layer.

Figure 7. Compressional velocity versus depth for sonobuoy stations in Anadyr and Navarin basins. Linear regression fit to data points in Anadyr basin is nearly indistinguishable from the fit to data in Navarin basin. Note that the relations between depth and velocity are based on refraction events from the top of layers. The expressions were not used in constructing Figure 15, where depth versus travel time for reflection events are calculated from the midpoint in a layer, not its top. Coefficients of determination for the regression lines from Navarin and Anadyr basins are 0.855 and 0.942, respectively.
and Anadyr basins are 0.855 and 0.942, respectively.

Figure 8. Compressional velocity versus depth from section B-B', onshore Anadyr basin, compared with best fits to sonobuoy velocities from offshore Anadyr and Navarin basins (Fig. 5).

Figure 9. Gravity and magnetic profiles and interpretative drawing of 24-channel seismic-reflection line #11

across Anadyr and Kresta basins. For location of profile see Figure 2. Travel time, in seconds, in two-way time. Detailed segment X-X' shown in Figure 10.

Figure 10. Twenty-four-channel seismic-reflection records used in constructing part of interpretative drawing shown in Figure 9.

Figure 11. Gravity and magnetic profiles and interpretative drawing of 24-channel seismic-reflection line #12 across Anadyr basin and ridge. For location of profile see Figure 2. Sono. 173 refers to sonobuoy station #173 (see Fig. 5).

Figure 12. Gravity and magnetic profiles and interpretative drawing of 24-channel seismic-reflection line #10 across Anadyr and Kresta basins. For location of profile see Figure 2.

Figure 13. Gravity and magnetic profiles and interpretative drawing of 24-channel seismic-reflection line #13 across Anadyr ridge and basin. For location of profile see Figure 2.

Figure 14. Gravity profile and interpretative drawing of 24-channel seismic-reflection line #9 across Navarin basin. For location of profile see Figure 2.

Figure 15. Structure-contour map of total sediment accumulation above and below the b reflector section. Procedure used to convert two-way travel time on seismic-reflection records to depths in kilometers is a generalized velocity function: $D = 1.266t + 1.033t^2 - 0.117t^3$, where D = depth or thickness in km and t = one-way travel time. Albers equal-area projection.

Figure 16. Isopach contours on top of the b reflector or pre-Cenozoic(?) section in offshore Anadyr basin (right half of figure from this study). Contours on left side of figure, mostly onshore, are on top of pre-Late Cretaceous rocks and are adopted from Dolzhanskiy et al. (Horizon d, Fig. 1, 1966), Burlin et al. (1974), and McLean (1979). The d horizon of Dolzhanskiy et al. (1966) has a refraction velocity of 4800 to 5200 m/s, whereas our b horizon has a refraction velocity of 4340 to 4780 m/s. Without offshore wells in Anadyr basin, we are unable to refine our interpretations to match the published Soviet contour maps accurately, which are based in part on 20 wells that were drilled in Anadyr basin.

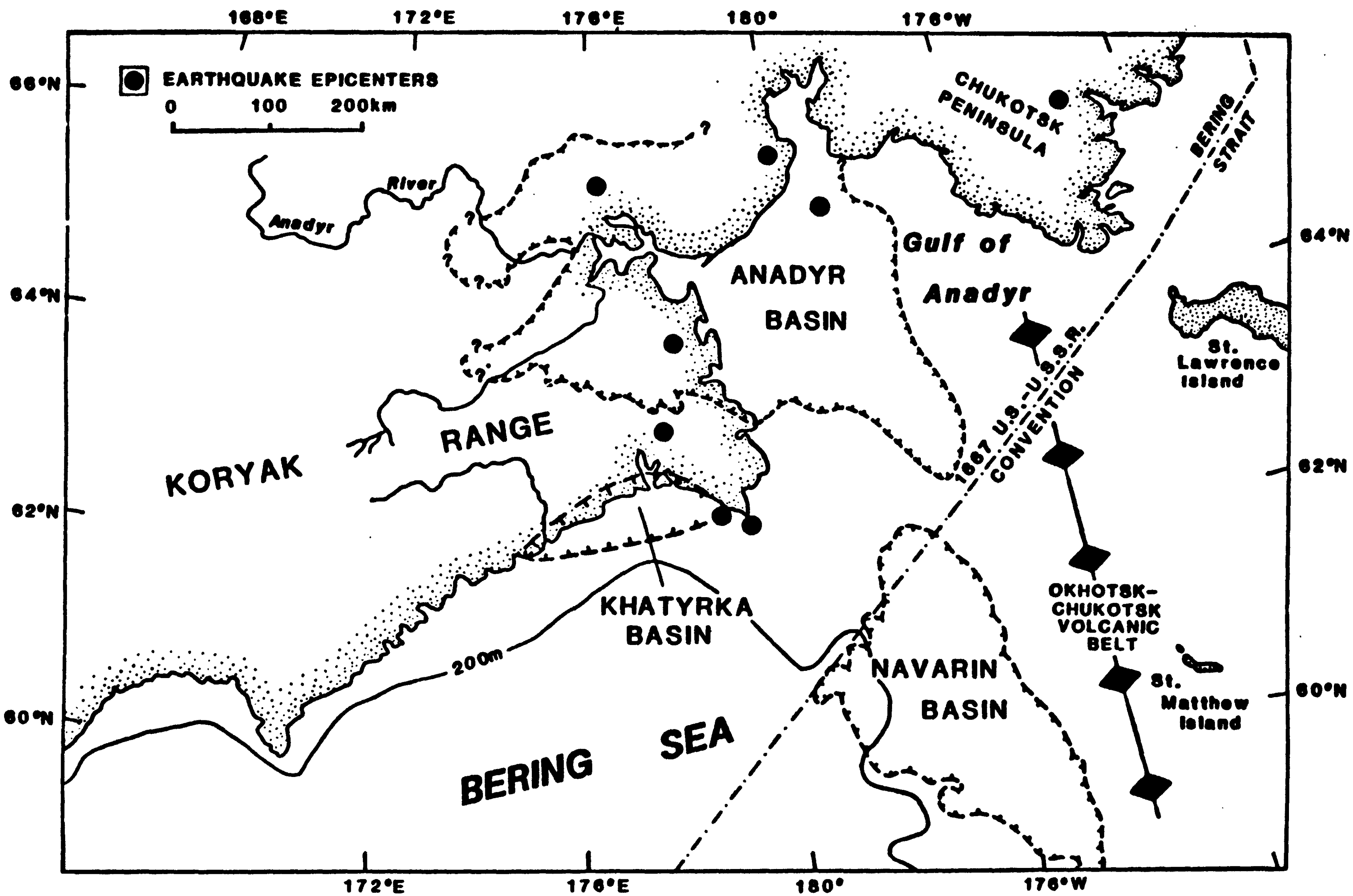

EARTHQUAKE EPICENTERS
0 100 200km
168°E
172°E
176°E
180°
176°W
66°N
64°N
62°N
60°N
Anadyr River
KORYAK RANGE
ANADYR BASIN
Gulf of Anadyr
CHUKOTSK PENINSULA
BERING STRAIT
1867 U.S.-U.S.S.R. CONVENTION
St. Lawrence Island
OKHOTSK-CHUKOTSK VOLCANIC BELT
St. Matthew Island
KHATYRKA BASIN
NAVARIN BASIN
200m
BERING SEA

Figure 1

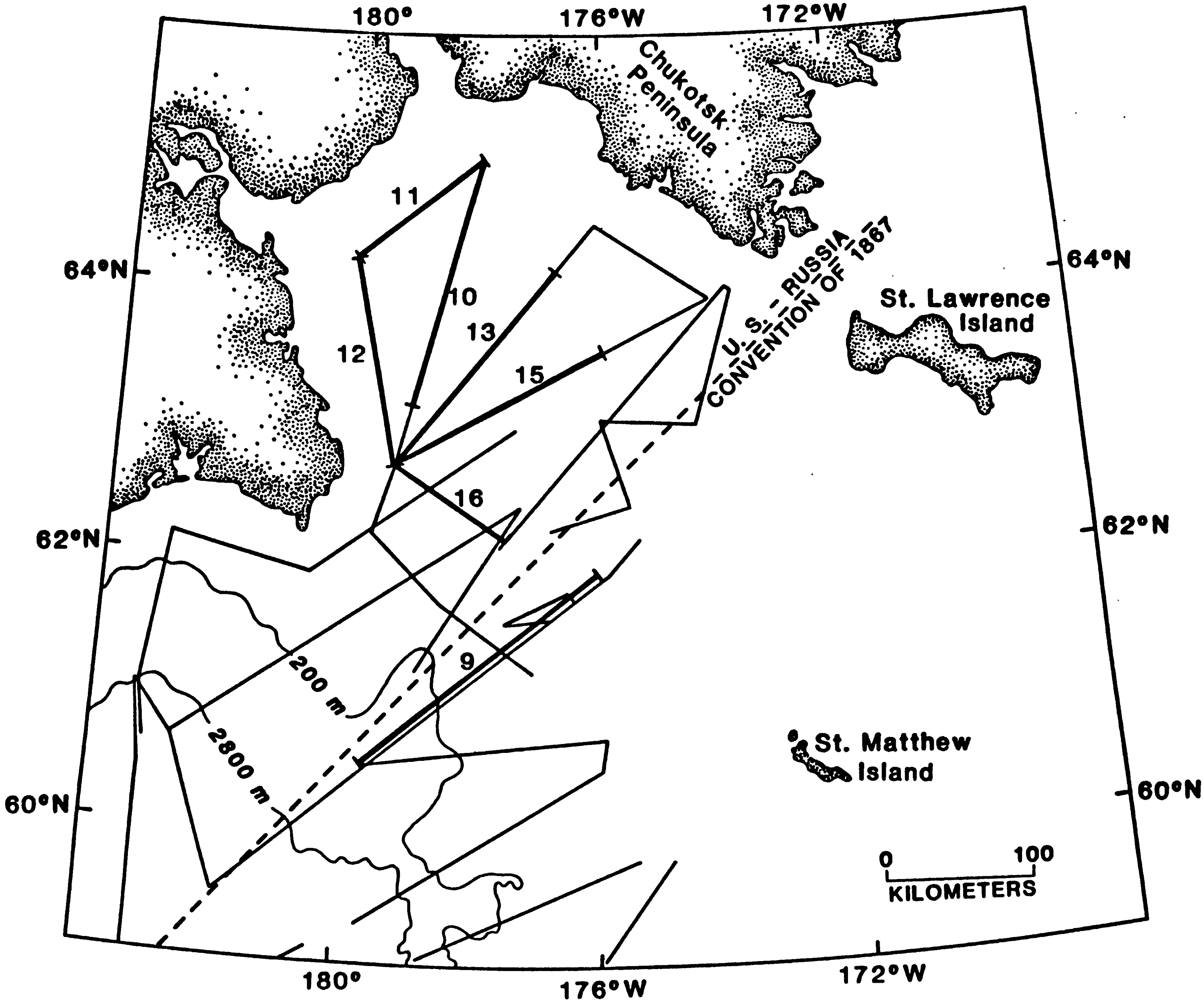
180°
176°W
172°W
Chukotsk Peninsula
64°N
62°N
60°N
St. Lawrence Island
U.S. - RUSSIA CONVENTION OF 1867
11
10
12
13
15
16
9
200 m
2800 m
St. Matthew Island
0
100
KILOMETERS

Figure 2

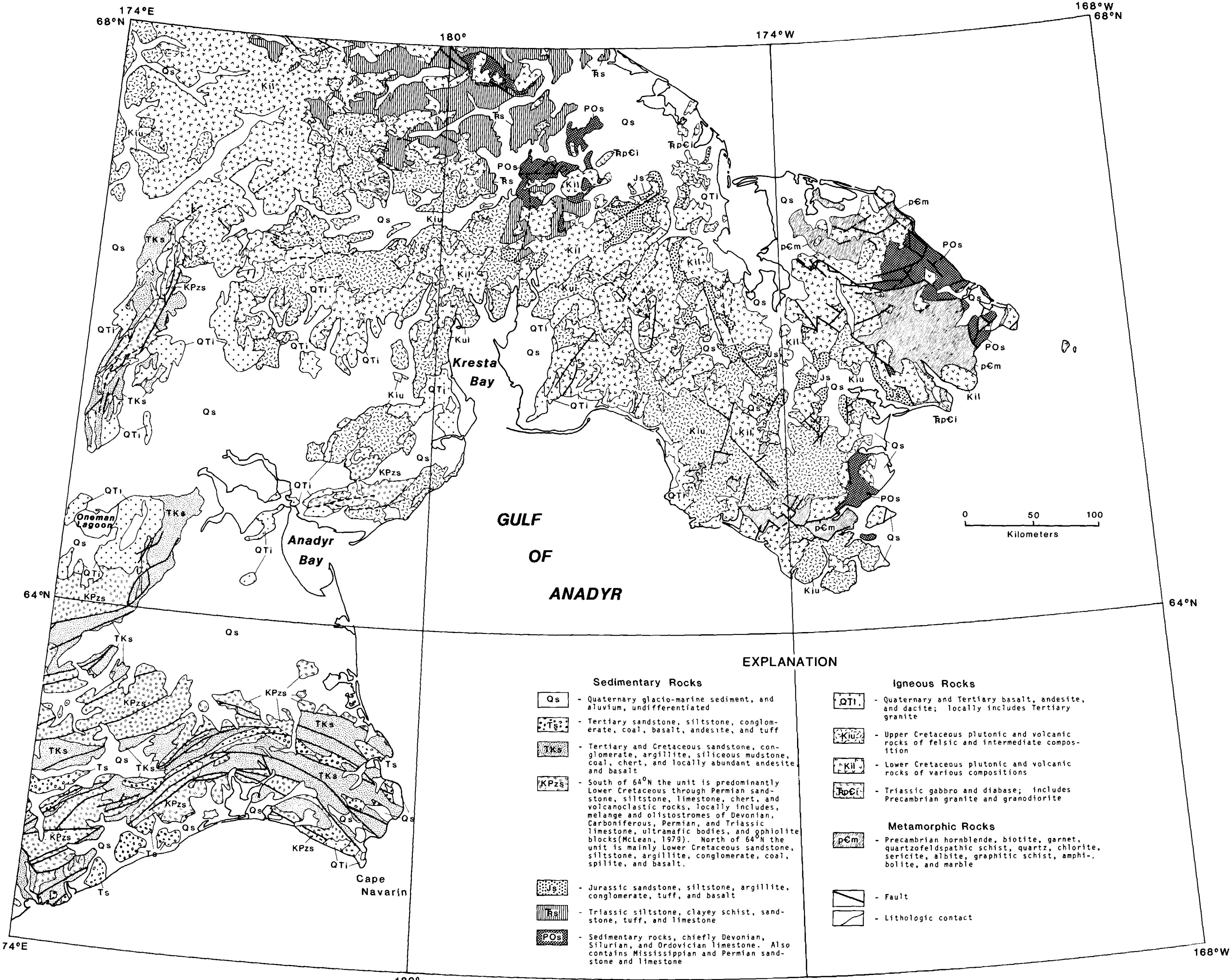
GULF
OF
ANADYR
Kresta Bay
Anadyr Bay
Oneman Lagoon
Cape Navarin
Kilometers
0
50
100
EXPLANATION
Sedimentary Rocks
Qs - Quaternary glacio-marine sediment, and aluvium, undifferentiated
Ts - Tertiary sandstone, siltstone, conglomerate, coal, basalt, andesite, and tuff
TKs - Tertiary and Cretaceous sandstone, conglomerate, argillite, siliceous mudstone, coal, chert, and locally abundant andesite and basalt
KPzs - South of 64°N the unit is predominantly Lower Cretaceous through Permian sandstone, siltstone, limestone, chert, and volcanoclastic rocks, locally includes, melange and olistostromes of Devonian, Carboniferous, Permian, and Triassic limestone, ultramafic bodies, and ophiolite blocks(McLean, 1979). North of 64°N the unit is mainly Lower Cretaceous sandstone, siltstone, argillite, conglomerate, coal, spilite, and basalt.
Js - Jurassic sandstone, siltstone, argillite, conglomerate, tuff, and basalt
Ћs - Triassic siltstone, clayey schist, sandstone, tuff, and limestone
POs - Sedimentary rocks, chiefly Devonian, Silurian, and Ordovician limestone. Also contains Mississippian and Permian sandstone and limestone
Igneous Rocks
QTi - Quaternary and Tertiary basalt, andesite, and dacite; locally includes Tertiary granite
Kiu - Upper Cretaceous plutonic and volcanic rocks of felsic and intermediate composition
Kil - Lower Cretaceous plutonic and volcanic rocks of various compositions
Ћp€i - Triassic gabbro and diabase; includes Precambrian granite and granodiorite
Metamorphic Rocks
p€m - Precambrian hornblende, biotite, garnet, quartzofeldspathic schist, quartz, chlorite, sericite, albite, graphitic schist, amphibolite, and marble
- Fault
- Lithologic contact

Figure 3

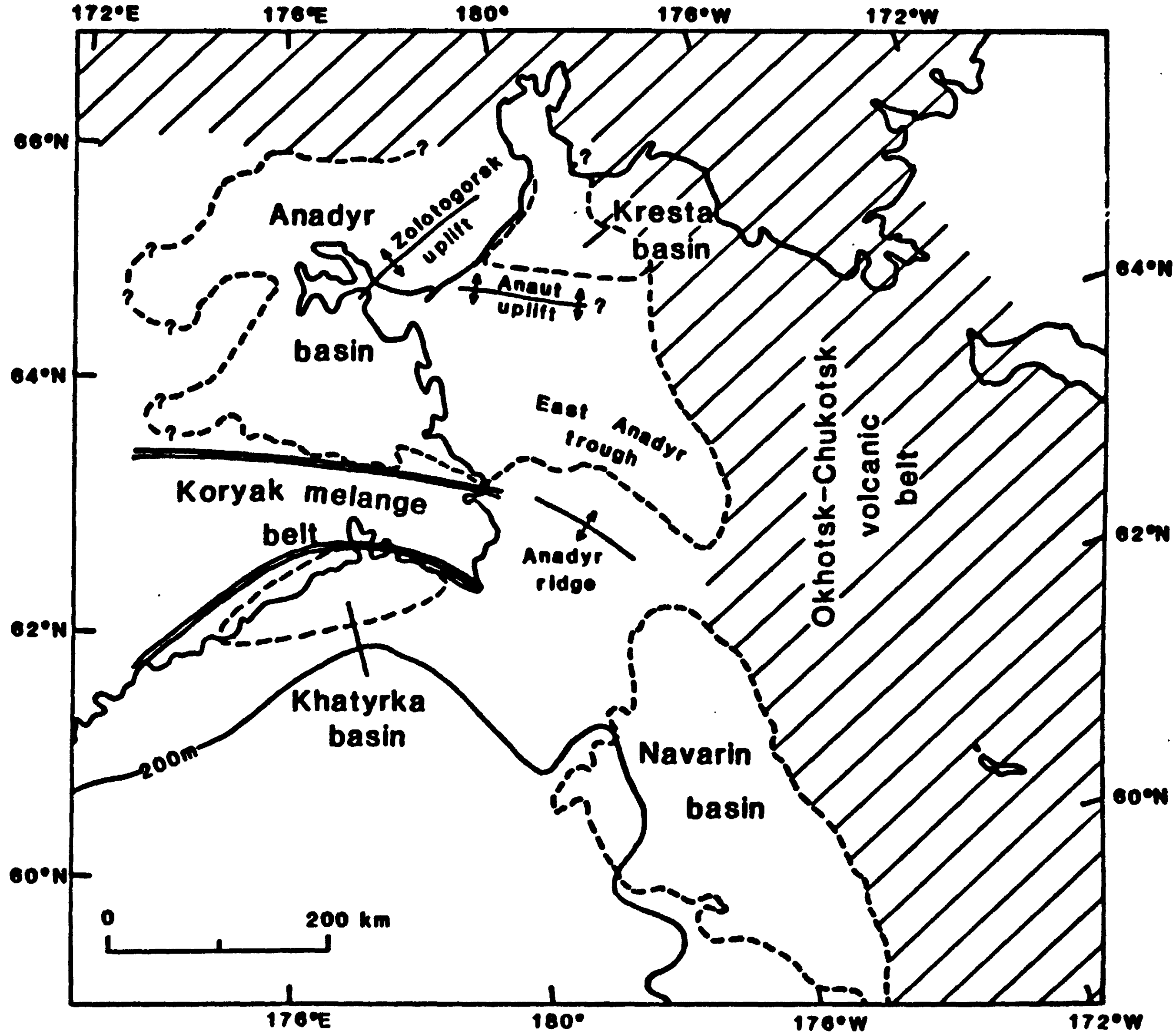
172°E
176°E
180°
176°W
172°W
66°N
64°N
62°N
60°N
Anadyr
basin
Zolotogorsk
uplift
Kresta
basin
Anaut
uplift
East
Anadyr
trough
Okhotsk-Chukotsk
volcanic
belt
Koryak melange
belt
Anadyr
ridge
Khatyrka
basin
Navarin
basin
200m
0
200 km

Figure 4

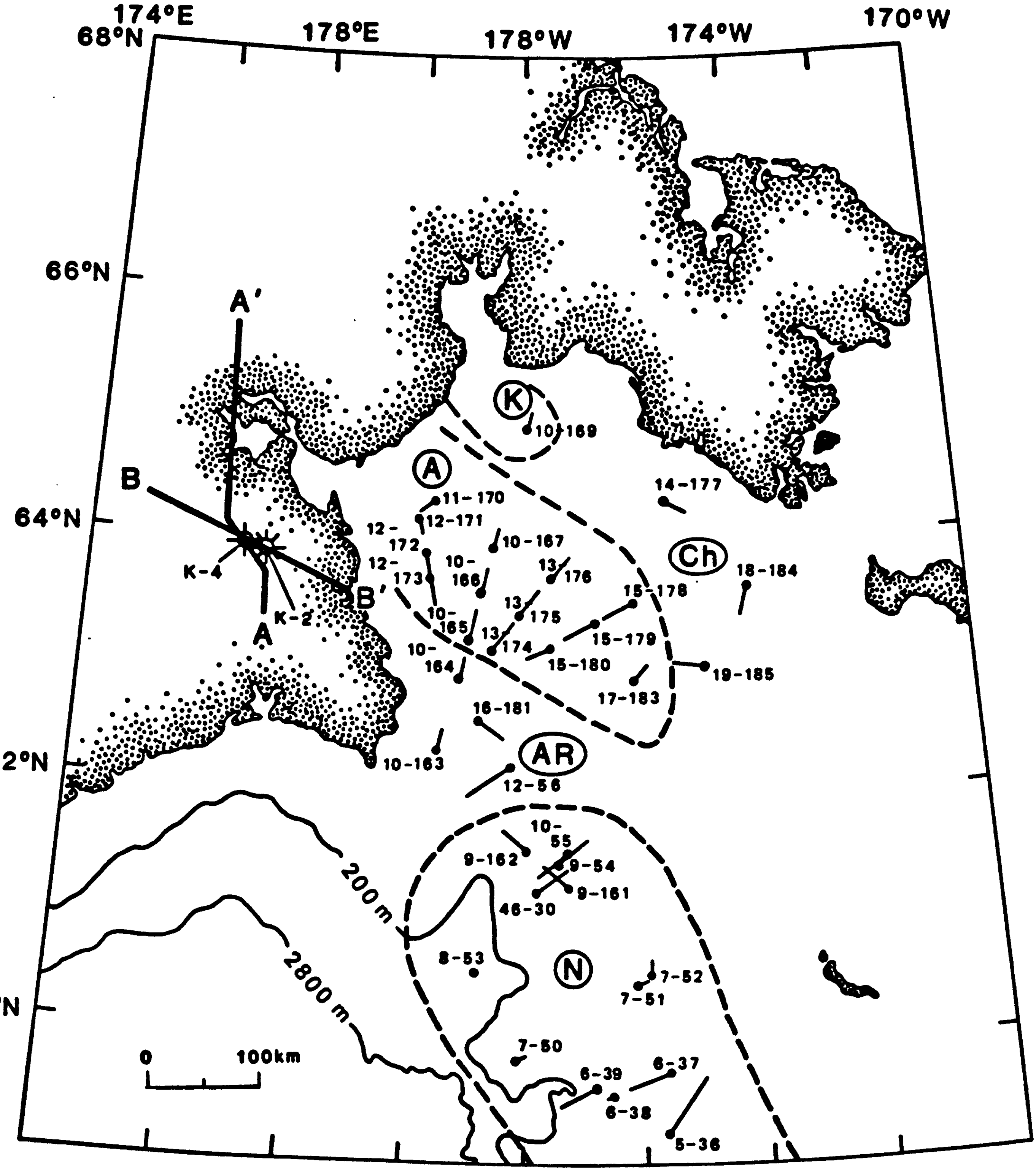
174°E
68°N
178°E
178°W
174°W
170°W
66°N
64°N
62°N
60°N
A'
A
B
B'
K-4
K-2
K
A
Ch
AR
N
10-169
14-177
11-170
12-171
12-172
10-167
12-173
10-166
13-176
18-184
15-178
10-165
13-175
15-179
13-174
10-164
15-180
19-185
17-183
16-181
10-163
12-56
10-55
9-162
9-54
9-161
46-30
200 m
2800 m
8-53
7-52
7-51
7-50
6-39
6-37
6-38
5-36
0
100km

Figure 5

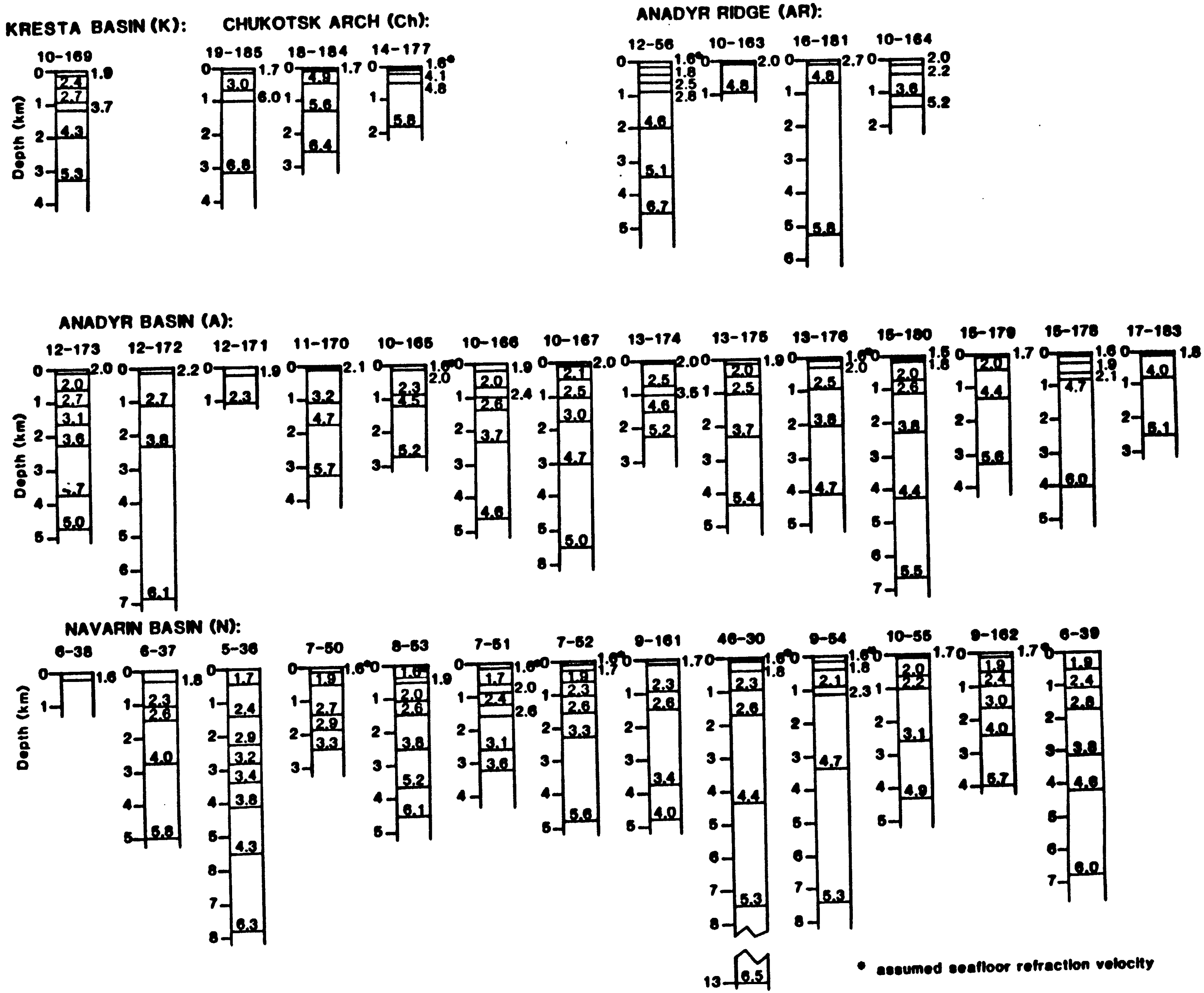
KRESTA BASIN (K):
10-169
CHUKOTSK ARCH (Ch):
19-185
18-184
14-177
ANADYR RIDGE (AR):
12-56
10-163
16-181
10-164
ANADYR BASIN (A):
12-173
12-172
12-171
11-170
10-165
10-166
10-167
13-174
13-175
13-176
15-180
15-179
15-178
17-183
NAVARIN BASIN (N):
6-38
6-37
5-36
7-50
8-53
7-51
7-52
9-161
46-30
9-54
10-55
9-162
6-39
Depth (km)
* assumed seafloor refraction velocity

Figure 6

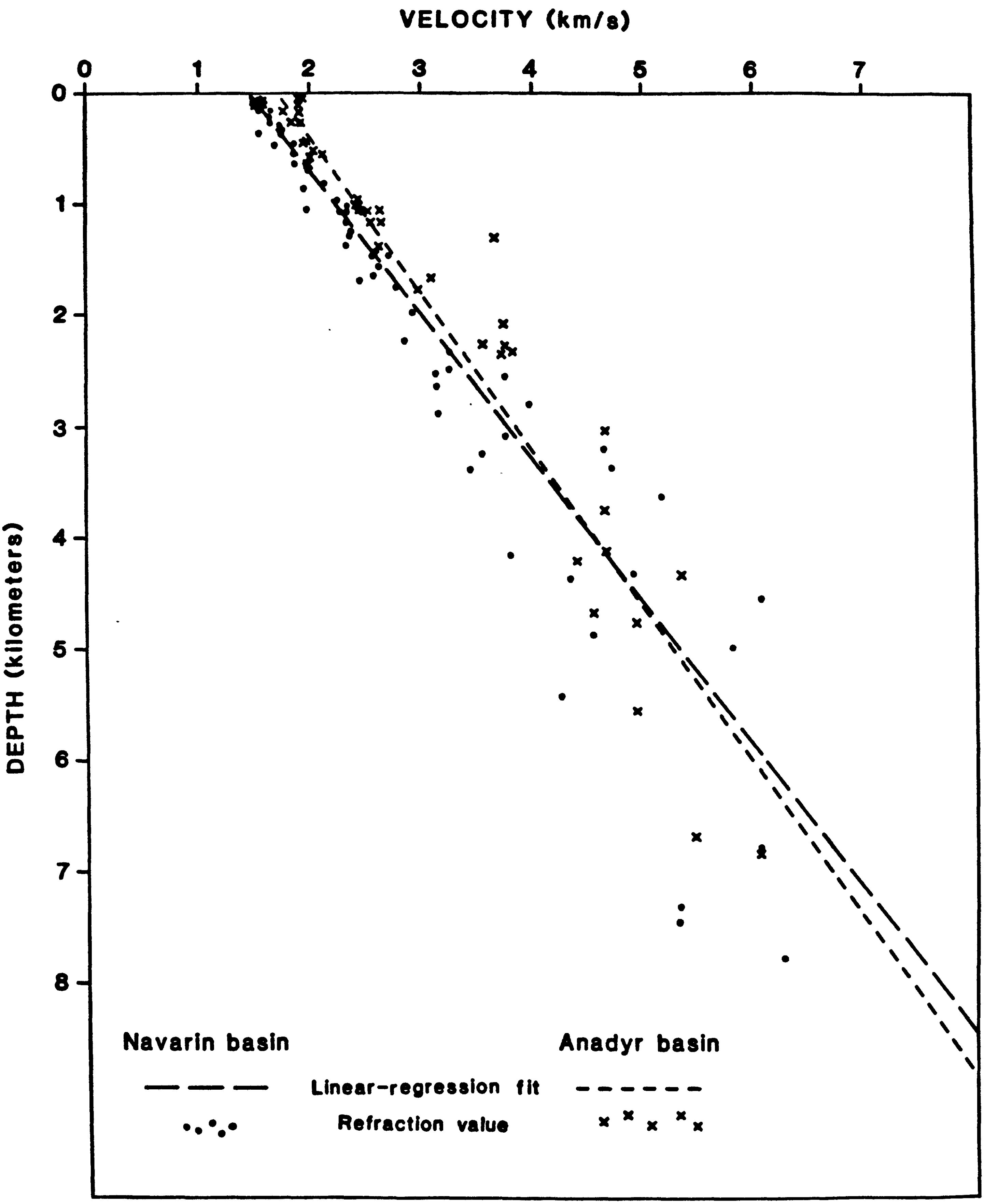
VELOCITY (km/s)
0
1
2
3
4
5
6
7
DEPTH (kilometers)
0
1
2
3
4
5
6
7
8
Navarin basin
Anadyr basin
Linear-regression fit
Refraction value

Figure 7

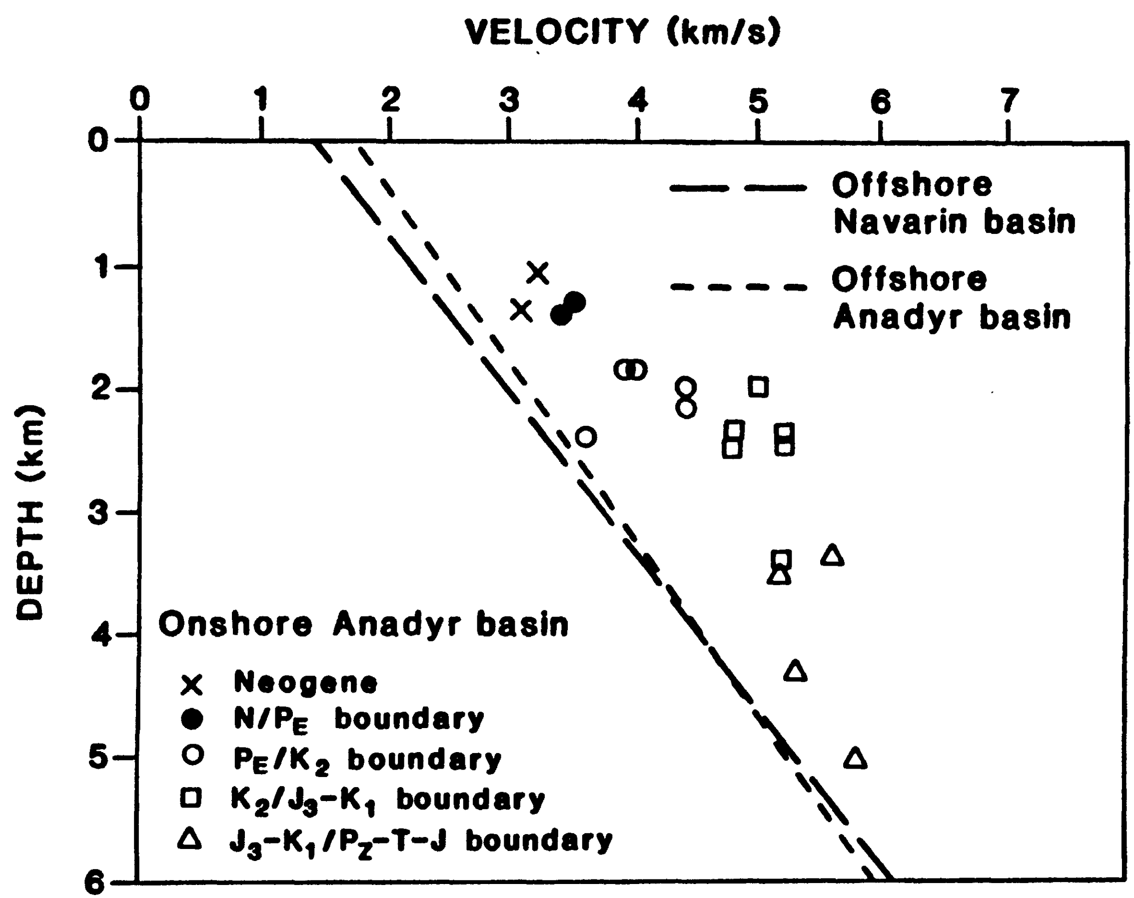
VELOCITY (km/s)
0
1
2
3
4
5
6
7
DEPTH (km)
0
1
2
3
4
5
6
Offshore Navarin basin
Offshore Anadyr basin
Onshore Anadyr basin
Neogene
N/P_E boundary
P_E/K_2 boundary
K_2/J_3-K_1 boundary
J_3-K_1/P_Z-T-J boundary

Figure 8

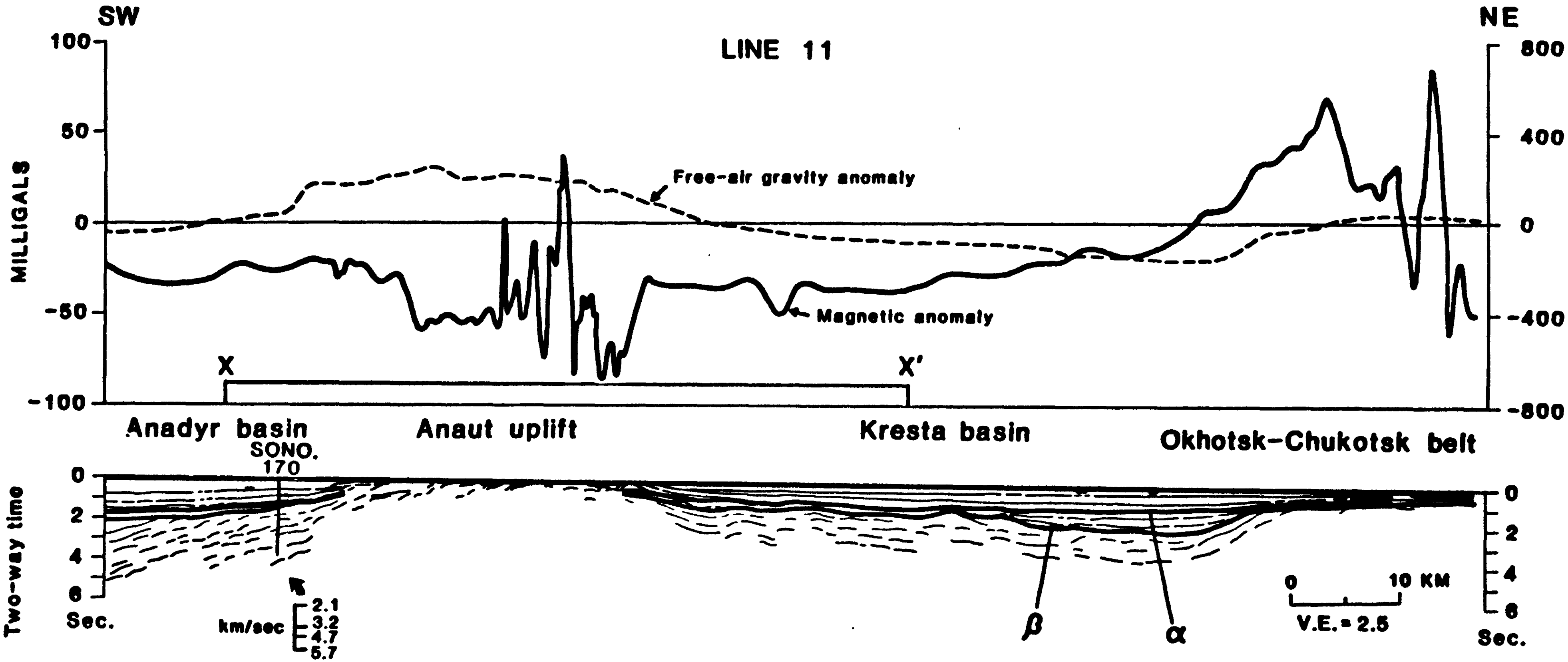
SW
NE
LINE 11
MILLIGALS
GAMMAS
100
50
0
-50
-100
800
400
0
-400
-800
Free-air gravity anomaly
Magnetic anomaly
X
X'
Anadyr basin
Anaut uplift
Kresta basin
Okhotsk-Chukotsk belt
SONO.
170
Two-way time
0
2
4
6
Sec.
km/sec
2.1
3.2
4.7
5.7
β
α
0
10 KM
V.E. = 2.5

Figure 9

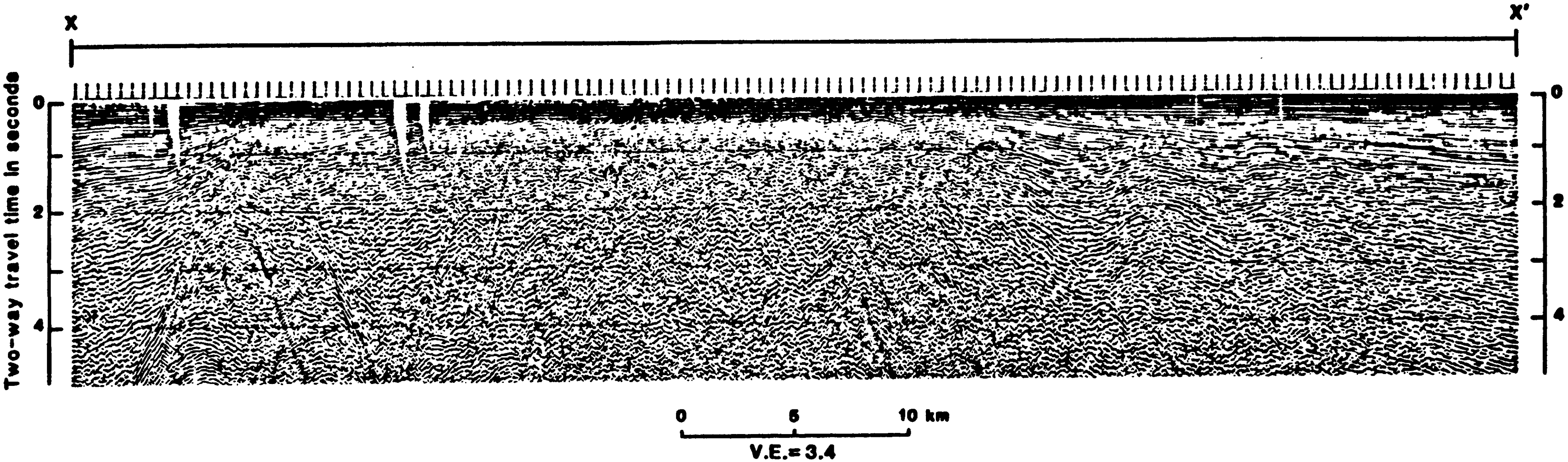

Figure 10

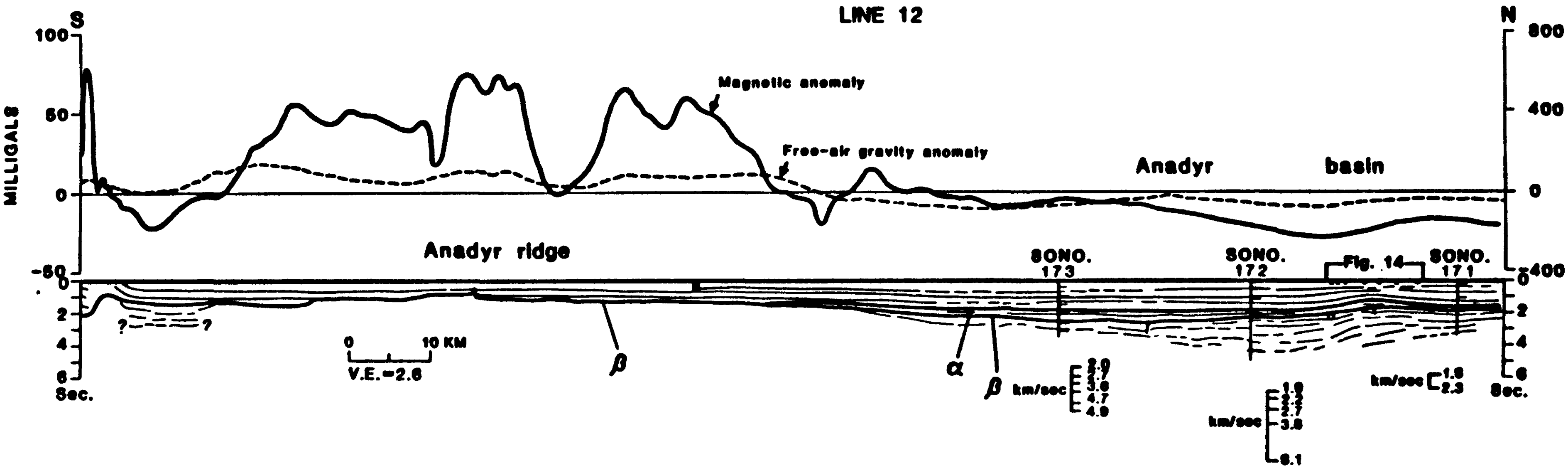
LINE 12
S
N
MILLIGALS
GAMMAS
Magnetic anomaly
Free-air gravity anomaly
Anadyr ridge
Anadyr basin
SONO. 173
SONO. 172
SONO. 171
Fig. 14
0 10 KM
V.E.=2.6
Sec.
α
β
km/sec

Figure 11

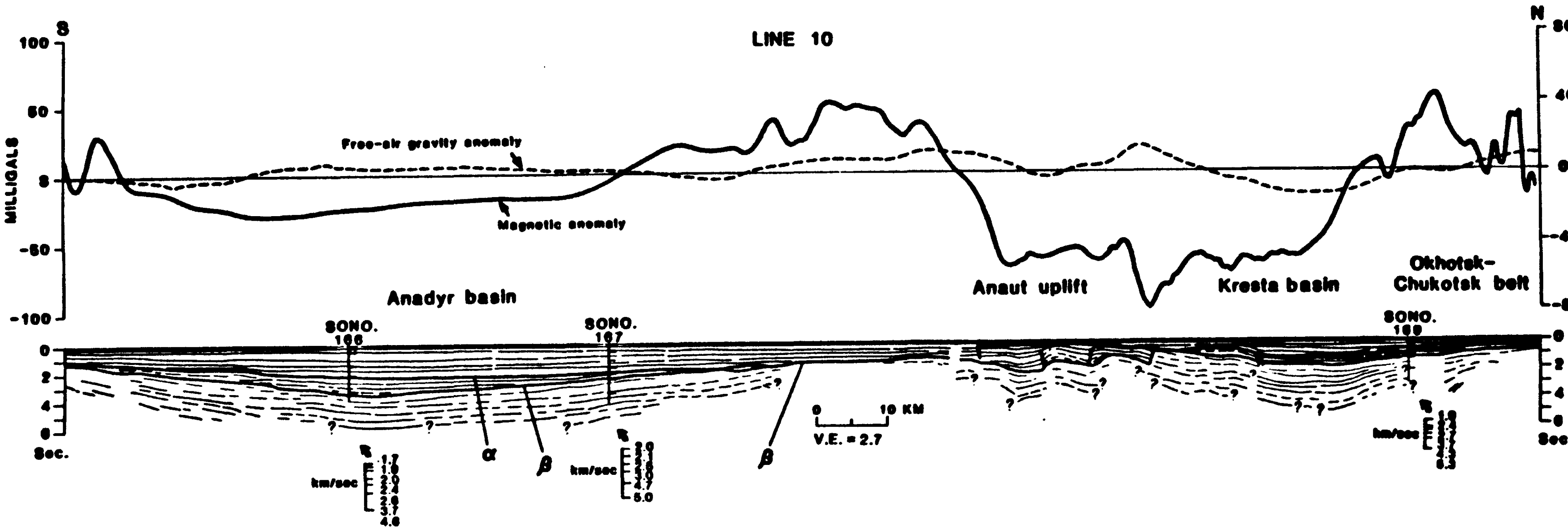
LINE 10
S
N
MILLIGALS
GAMMAS
Free-air gravity anomaly
Magnetic anomaly
Anadyr basin
Anaut uplift
Kresta basin
Okhotsk-
Chukotsk belt
SONO.
166
SONO.
167
SONO.
169
km/sec
Sec.
0
10 KM
V.E. = 2.7
α
β
β

Figure 12

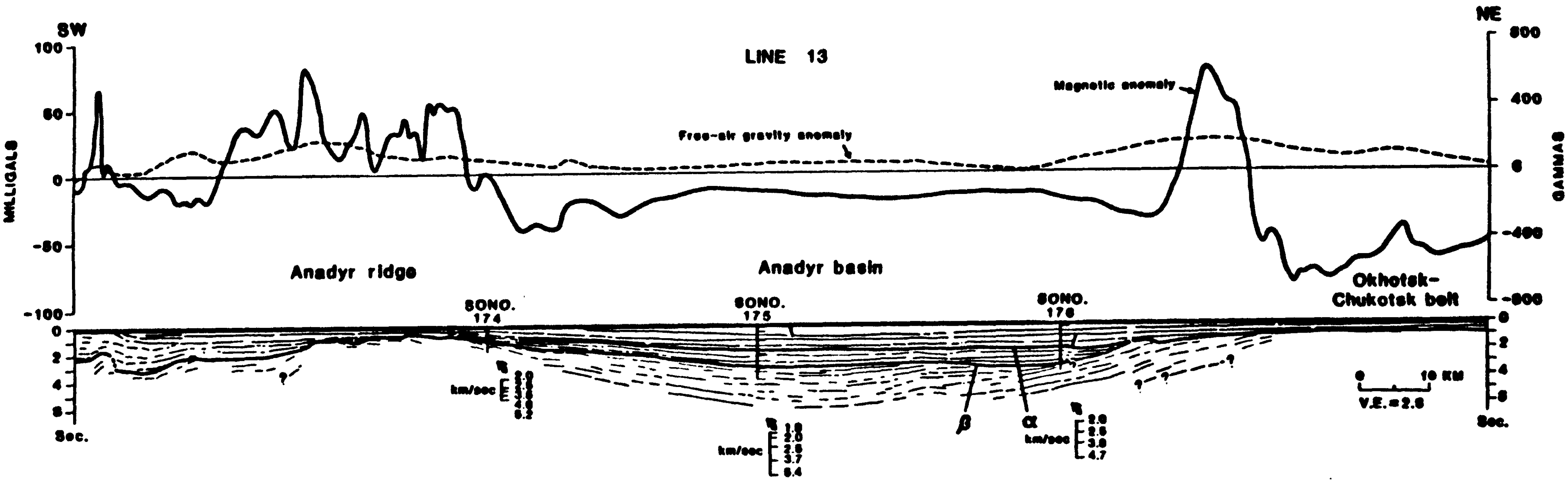
SW
NE
LINE 13
MILLIGALS
GAMMAS
100
50
0
-50
-100
800
400
0
-400
-800
Magnetic anomaly
Free-air gravity anomaly
Anadyr ridge
Anadyr basin
Okhotsk-
Chukotsk belt
SONO.
174
SONO.
175
SONO.
176
km/sec
1.8
2.0
2.6
3.7
5.4
km/sec
2.0
2.5
3.8
4.7
β
α
0
10 KM
V.E.=2.8
Sec.
Sec.

Figure 13

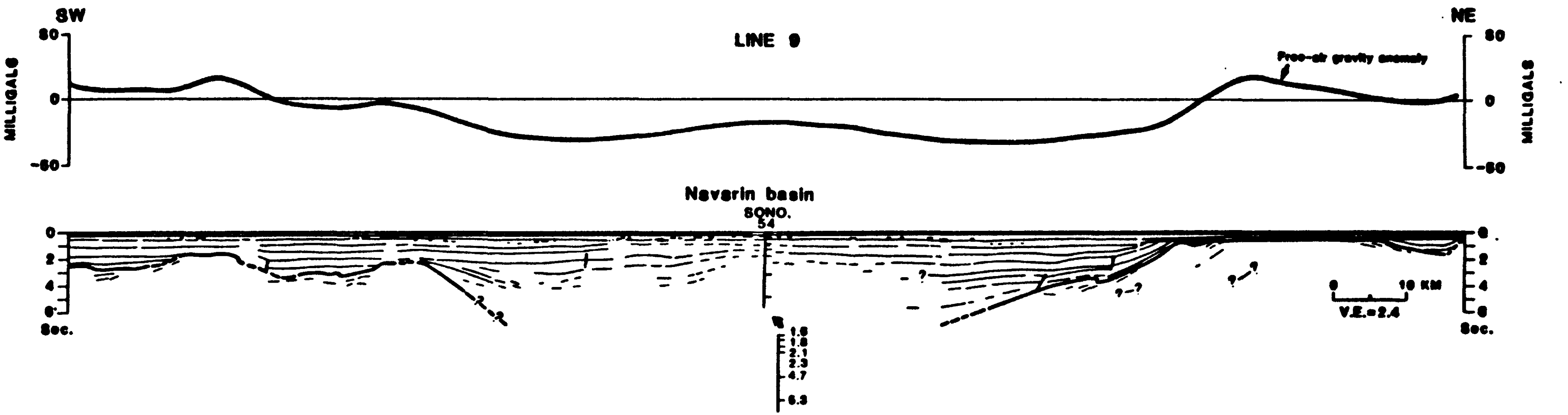
LINE 9
SW
NE
MILLIGALS
50
0
-50
Free-air gravity anomaly
Navarin basin
SONO.
54
0
2
4
6
Sec.
0
10 KM
V.E.=2.4
1.8
1.8
2.1
2.3
4.7
6.3

Figure 14

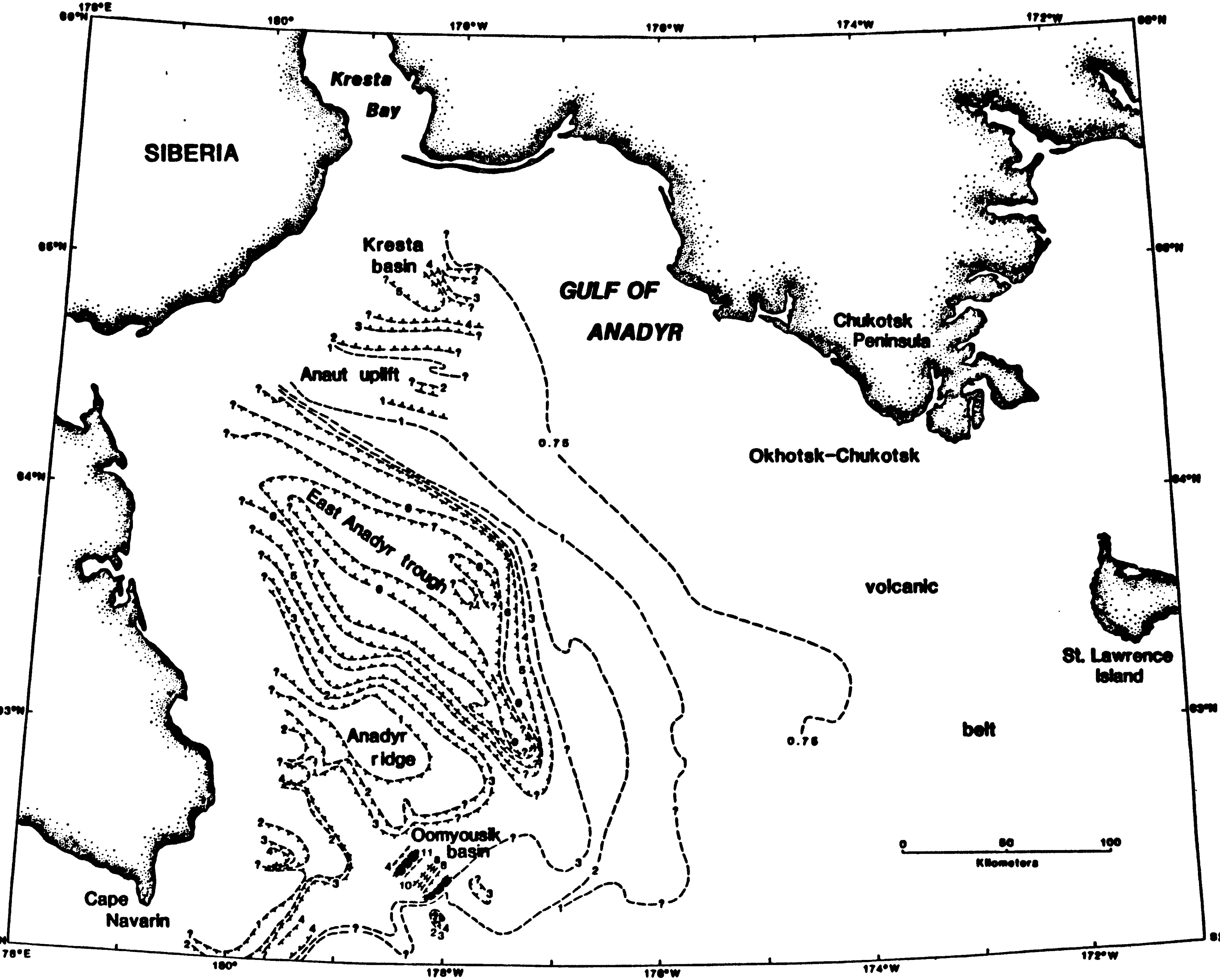
SIBERIA
Kresta Bay
Kresta basin
GULF OF ANADYR
Chukotsk Peninsula
Anaut uplift
Okhotsk-Chukotsk volcanic belt
East Anadyr trough
St. Lawrence Island
Anadyr ridge
Oomyousik basin
Cape Navarin
0 50 100
Kilometers
0.75

Figure 15

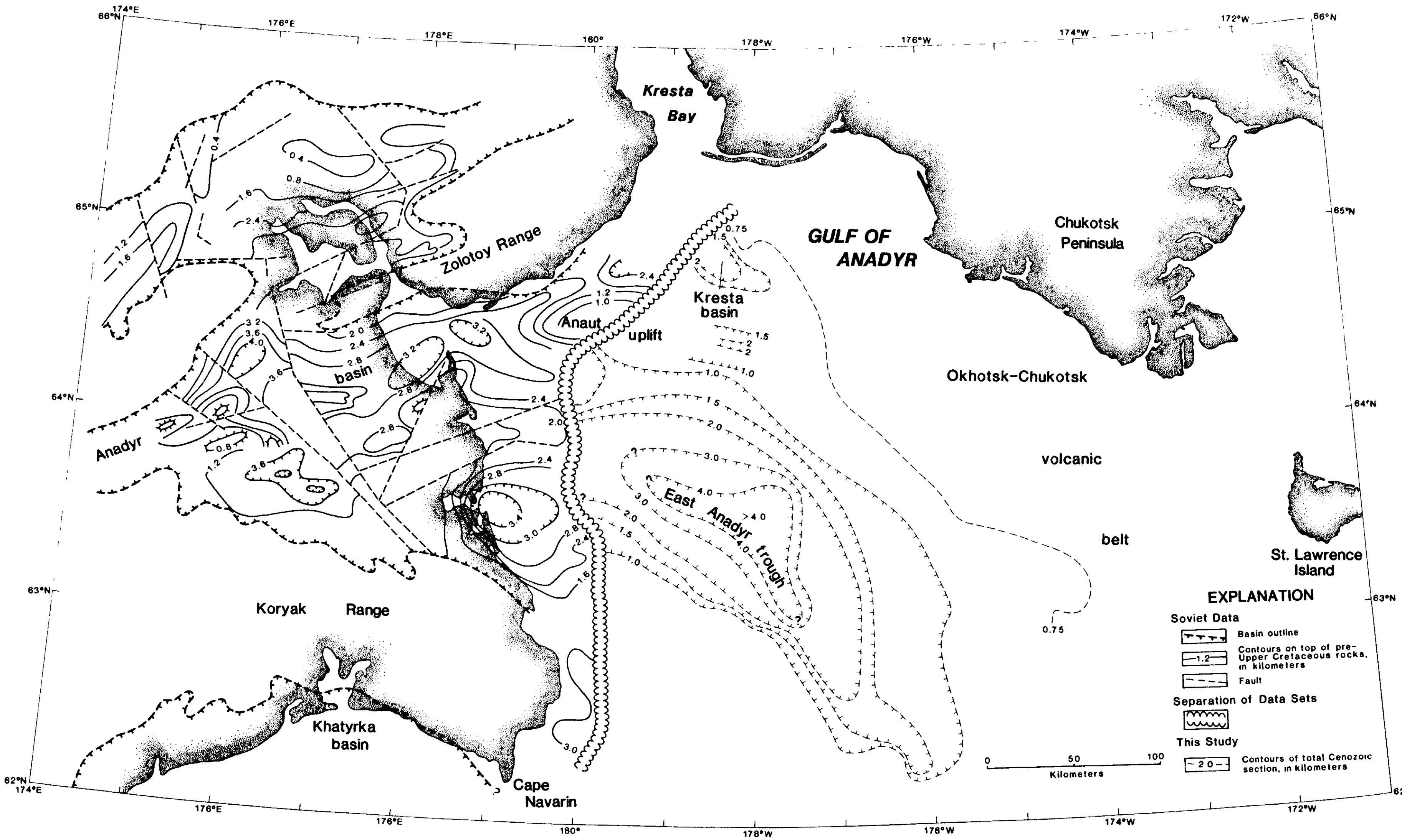

Kresta Bay
GULF OF ANADYR
Chukotsk Peninsula
Zolotoy Range
Anaut uplift
Kresta basin
Okhotsk-Chukotsk volcanic belt
East Anadyr trough
Anadyr basin
Koryak Range
Khatyrka basin
Cape Navarin
St. Lawrence Island
EXPLANATION
Soviet Data
Basin outline
Contours on top of pre-Upper Cretaceous rocks, in kilometers
Fault
Separation of Data Sets
This Study
Contours of total Cenozoic section, in kilometers
0 50 100
Kilometers

Figure 16

PART II

PRELIMINARY GEOLOGICAL AND GEOPHYSICAL STUDIES OF THE BERING SEA SHELF, INCLUDING NAVARIN BASIN, DURING 1982

The following text is abstracted from a U.S. Geological Survey report (Cooper and Marlow, 1983) that summarizes the results of the 1982 field season work on the Bering Shelf.

During July 1982, approximately 2,900 nautical miles of geophysical data as well as rocks from 14 dredge stations were collected aboard the R/V S.P. LEE from the Bering Sea shelf (Fig. 1). The first phase of the cruise (L9-82-BS) was a government- industry cooperative project (GICORP) with the Center for Marine Crustal Studies of the Gulf Oil Corporation; the objectives were to collect data on deep crustal structure from seismic refraction profiles and to use these data for designing a future two-ship multifold seismic-reflection/refraction survey of the shelf. During this phase, 52 sonobuoys and approximately 1,500 nm. of multichannel seismic-reflection, gravity, magnetic, and bathymetric data were collected. The second phase included dredging the outer edge of the continental shelf and collecting geophysical data between dredge stations.

Phase 1 - Deep crustal refraction studies

Unreversed seismic refraction profiles were recorded to offsets of 35-45 km using U.S Navy and commercial sonobuoys. A large volume (1,300-2,250 cu. in.) airgun array, fired at 50-m intervals, provided the seismic source. Preliminary analysis of the sonobuoy data has been done by the slope-intercept technique has provided crustal velocity-versus-depth information to depths of 12-14 km (/ig. 2). The technique assumes that discrete layers of uniform velocity are present, an assumption that is not valid over long distances in areas of complex geology. Because only straight segments of the refraction arrivals have been used, the velocities and thicknesses of crustal layers close to the sonobuoy location are probably reliable. Future processing of the refraction data with intercept-ray parameter and ray-tracing methods will give better definition of the variations of velocity with depth and with horizontal distance along the transect.

Several preliminary observations and conclusions can be made from two transects shown in Figure 2:

1. Crustal layers with high velocities (6.7-7.6 km/sec) are found at shallow depths (5-9 km) beneath large areas of the inner Bering shelf. High-velocity igneous and metamorphic rocks, such as layered gabbros, ultramafic rocks, schists, and amphibolites, occur near Hagemeister Island (transect 4-5; Hoare and Coonrad,1977). These or similar rocks may underlie

the inner shelf near St. Matthew Island (transect 6-9) and be part of the igneous-metamorphic belt that is believed to extend across the shelf from Alaska to Siberia (Marlow and others, 1976)

2. Large crustal depressions are associated with Bristol and Navarin basins, and these depressions may be filled with as much as 6 km and 13 km, respectively, of Cenozoic and Mesozoic strata.

3. An abrupt change in magnetic and gravity anomalies occurs along transect 6-9 on the eastern side of Navarin Basin; the change is seen in other profiles across the region and may mark the fault-controlled juxtaposition of two distinct terranes: a predominantly igneous-metamorphic terrane beneath the inner shelf (Nunivak arch) and a predominantly sedimentary terrane beneath Navarin Basin.

4. Kuskokwim Bay is underlain by a crustal depression that is filled with at least 5 km of rocks that have velocities (4.1-5.5 km/sec) similar to those for Mesozoic volcanic and sedimentary rocks sampled in the onshore Bethel well, 150 km to the northeast. The offshore section may be a continuation of the onshore Kuskokwim Basin and may extend to the eastern edge of Navarin Basin. Other small depressions, between Nunivak and St. Matthew Island, are suggested by undulations in the gravity data and by shallow high-velocity refractors; these depressions may also contain Mesozoic sedimentary and volcanic rocks. Similar Mesozoic rocks may occur beneath the Cenozic fill of Navarin Basin, as horizons with similar velocities are found in the basin

5. Large magnetic anomalies of the inner shelf fall into two general categories: those of very high-amplitude, high-frequency (St. Matthew Island), and those of lesser amplitude and broader wavelength (Kuskokwim Bay). The first category may be caused by near-seafloor intrusive and volcanic rocks (Hagemeister Island area), as well as volcanic flows (St. Matthew Island); the second category probably results from more deeply buried volcanic piles (Kuskokwim Bay) and intra-basement structures. Similar magnetic anomalies are not found in Navarin Basin which suggests that either Navarin Basin is not underlain by a plutonic-volcanic basement terrane or that the magnetic basement rocks are too deeply buried or thermally altered to produce large magnetic anomalies.

Phase 2 - Geological studies

Prior to this study, dredge sampling along the northern Bering Sea shelf edge (Marlow and others, 1979) recovered upper Jurassic and upper Cretaceous limestone and sandstone as well as lower Tertiary basalt, limestone, and mudstone from the acoustic basement; these rocks are overlain by Cenozoic mudstone, sandstone, limestone, and tuff. During the 1982 cruise, dredge samples were collected at fourteen nearby localities along the outer shelf edge (Fig. 1). Rocks from beneath and above the prominent unconformity at the top of the acoustic basement surface were collected and analyzed.

Preliminary examination of the rock samples obtained during the 1982 cruise show that:

1. Limestone recovered at most dredge stations and throughout the sedimentary section is of secondary origin and was not deposited originally as carbonate sediment.

2. A pinnacle of fresh basaltic rocks, discovered on the shelf in shallow water, cross-cuts and overlies the flat-lying sedimentary section at the shelf edge. These rocks may be syngenetic with Quaternary volcanic flows on Nunivak and the Pribilof Islands.

3. Rocks with opaline silica(opal-CT) and quartz were recovered from the lower parts of the sedimentary section and may be the result of diagenesis of the overlying diatomaceous (opal-A) mudstone and siltstone.

4. Conglomerate, found at several sites and presumed to be from the unconformity directly above basement, may be of Oligocene age, based on its similarity to a sample recovered nearby in 1970 (Marlow and others, 1976).

5. Volcanic and meta-igneous rocks, recovered from the basement in an area where a sample of Eocene (minimum age) basaltic andesite was obtained in 1978, do not appear to be widespread beneath the slope, based on magnetic and sample data; however, they may be more common beneath the shelf where refraction data indicate rocks having similar velocities (5.5-6.0 km/sec) are present.

6. Correlation of refraction and geologic data at the shelf edge (Fig. 3) indicates a sequence of presumably Neogene diatomaceous mudstone, sandstone, and limestone (1.6-4.5 km/sec) overlying an unconformity marked by conglomerate (4.9 km/sec) and underlain by other more highly indurated sedimentary and volcanic basement rocks (4.9-5.8 km/sec).

BIBLIOGRAPHY

Cooper, A.K. and Marlow, M.S., 1983, Preliminary results of geophysical and geologcial studies of the Bering Sea shelf during 1982, U.S. Geological Survey Open-file Report 83-322, 8 p.

Hoare, J.M. and Coonrad, W.L., 1977, New geologic map of the Goodnews-Hagemeister Island quadrangles region, Alaska: U.S. Geological Survey Circular 772-B, p. B50-B54.

Marlow, M.S., Scholl, D.W., Cooper, A.K. and Buffington, E.C., 1976, Structure and evolution of Bering Sea shelf south of St. Lawrence Island: American Association of Petroleum Geologists Bulletin, v. 60, p. 161-183.

Marlow, M.S., Cooper, A.K., Scholl, D.W., Vallier, T.L., and McLean, H., 1979, Description of dredge samples from the Bering Sea continental margin: U.S. Geological Survey Open-file report 79-1139, 5 p.

FIGURE CAPTIONS

Figure 1: Index map showing location of geophysical tracklines and geological sampling site for cruise L9-82-BS. Water depth in meters.

Figure 2: Interpretation of two geophysical transects across the Bering Sea shelf that show preliminary velocities (km/sec) and thicknesses for crustal layers, based on sonobuoy refraction profiles located on Figure 1.

Figure 3: Seismic-reflection profile showing rock types dredged along the profile and refraction velocities (km/sec) measured at a sonobuoy station 5 km from the end of the profile. See Figure 1 for location.

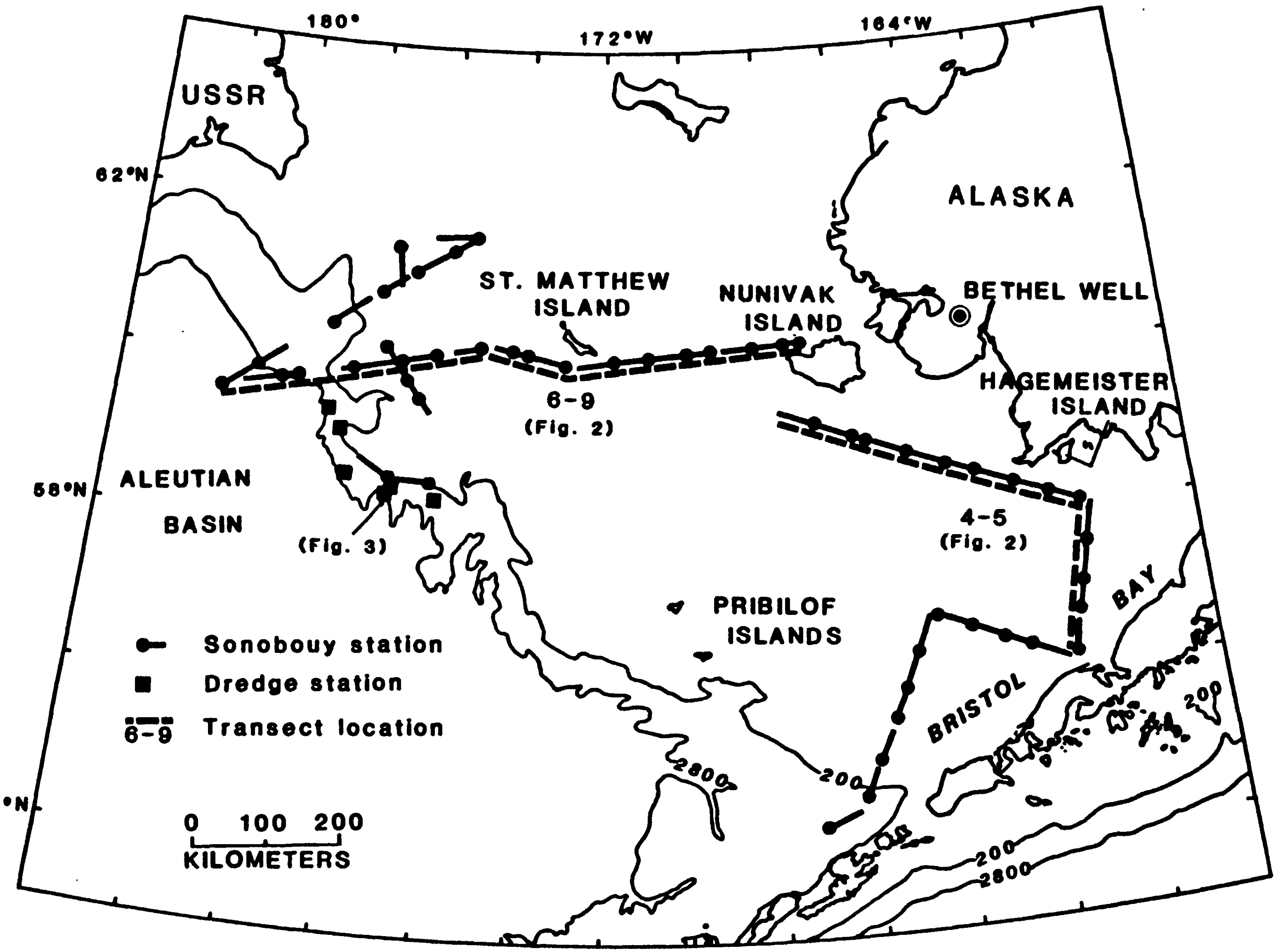
180°
172°W
164°W
62°N
58°N
54°N
USSR
ALASKA
ST. MATTHEW ISLAND
NUNIVAK ISLAND
BETHEL WELL
HAGEMEISTER ISLAND
6-9 (Fig. 2)
4-5 (Fig. 2)
ALEUTIAN BASIN
(Fig. 3)
PRIBILOF ISLANDS
BRISTOL BAY
200
2800
Sonobouy station
Dredge station
6-9 Transect location
0 100 200
KILOMETERS

Figure 1

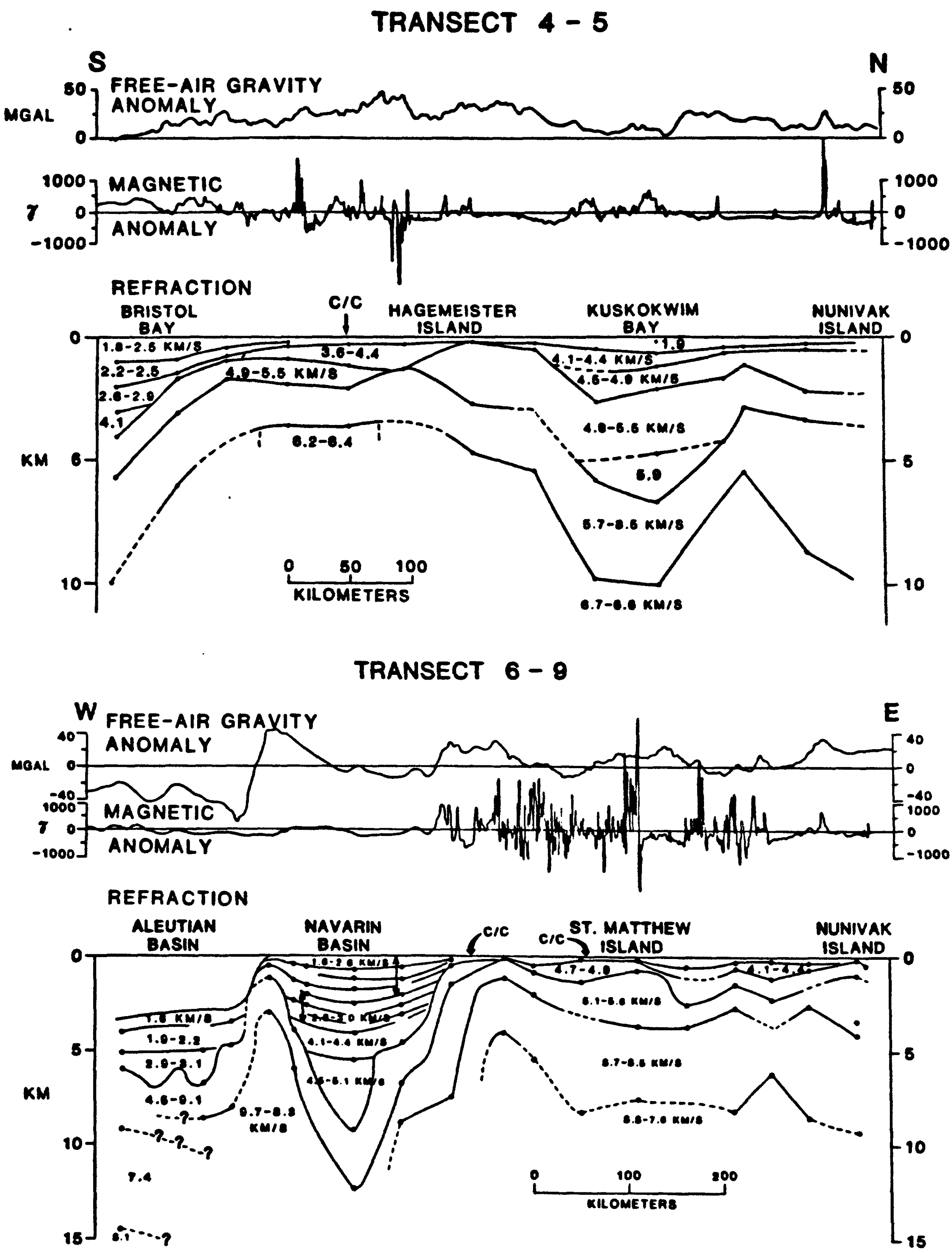
TRANSECT 4 - 5
S
N
FREE-AIR GRAVITY ANOMALY
MGAL
50
0
MAGNETIC ANOMALY
γ
1000
0
-1000
REFRACTION
BRISTOL BAY
C/C
HAGEMEISTER ISLAND
KUSKOKWIM BAY
NUNIVAK ISLAND
KM
0
5
10
1.8-2.5 KM/S
2.2-2.5
2.6-2.9
4.1
3.6-4.4
4.9-5.5 KM/S
6.2-6.4
1.9
4.1-4.4 KM/S
4.5-4.9 KM/S
4.8-5.5 KM/S
5.9
5.7-6.5 KM/S
6.7-6.8 KM/S
0 50 100
KILOMETERS
TRANSECT 6 - 9
W
E
FREE-AIR GRAVITY ANOMALY
MGAL
40
0
-40
MAGNETIC ANOMALY
γ
1000
0
-1000
REFRACTION
ALEUTIAN BASIN
NAVARIN BASIN
C/C
ST. MATTHEW ISLAND
NUNIVAK ISLAND
KM
0
5
10
15
1.8 KM/S
1.9-2.2
2.9-3.1
4.6-6.1
5.7-6.3 KM/S
7.4
8.1
4.1-4.4 KM/S
4.5-5.1 KM/S
4.7-4.9
5.1-5.6 KM/S
5.7-6.5 KM/S
6.6-7.0 KM/S
0 100 200
KILOMETERS

Figure 2

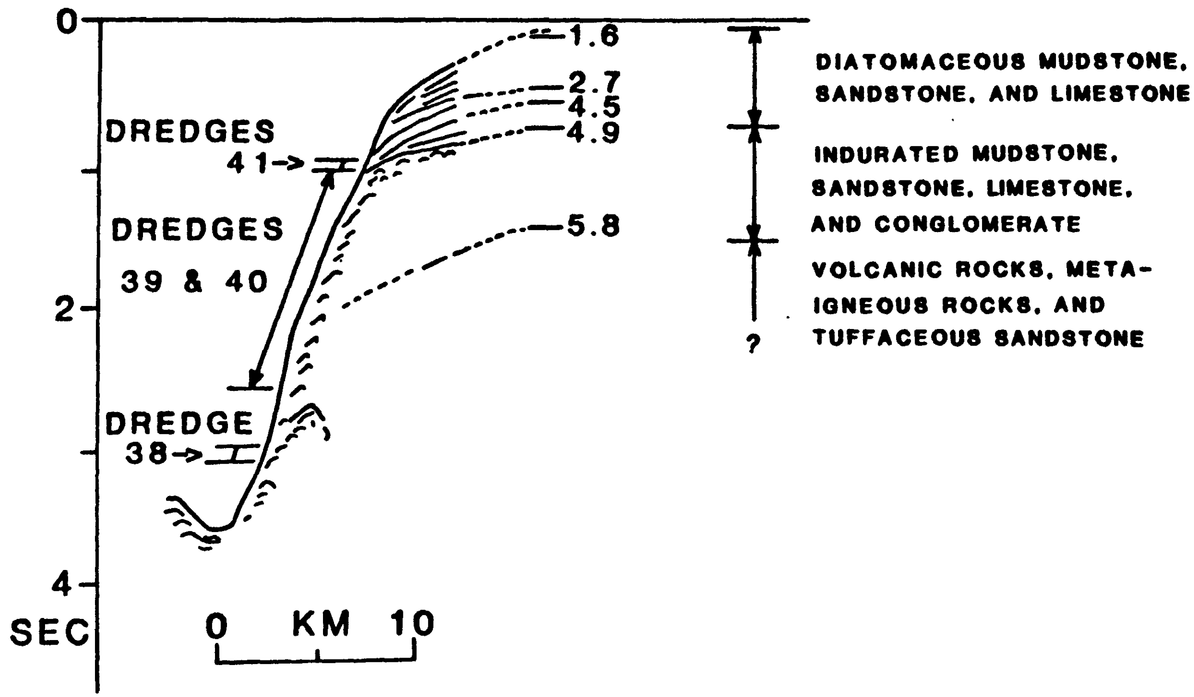
0
2
4
SEC
DREDGES
41->
DREDGES
39 & 40
DREDGE
38->
0 KM 10
1.6
2.7
4.5
4.9
5.8
?
DIATOMACEOUS MUDSTONE, SANDSTONE, AND LIMESTONE
INDURATED MUDSTONE, SANDSTONE, LIMESTONE, AND CONGLOMERATE
VOLCANIC ROCKS, META-IGNEOUS ROCKS, AND TUFFACEOUS SANDSTONE

Figure 3

PART III REGIONAL HAZARDS:

Mass Movement Features in the Head of Navarinsky Canyon, Bering Sea

ABSTRACT

Two types of morphologic features in the head of Navarinsky Canyon are attributed to mass movement of near-surface sediment. A series of pull-aparts is located downslope of large sand waves. These pull-aparts, possibly induced by liquefaction, affect the upper 5-10 m of sandy sediment (water depths 350-600 m) on a 1° slope. A hummocky elongate mound of muddy sand (water depths 550-800 m) contains chaotic internal reflectors to a subbottom depth of 30-40 m and possibly is the product of a shallow slide. We speculate that Holocene seismicity is the likely triggering mechanism.

INTRODUCTION

Mass movement has been an important process in the evolution of the world's continental margins [1-3]. As coverage of frontier areas is increased, so is knowledge of the various forms of mass movement that modify the continental slopes.

The purpose of this report is to illustrate and discuss two puzzling types of mass-movement features discovered in the head of Navarinsky Canyon, one of the largest (4,900-km^3 volume) of the large canyons incised into the continental margin of the Bering Sea [4,5] (Fig. 1).

The study area is a part of the Navarin basin province, a potential petroleum province that is scheduled for leasing in 1984. The Navarin basin contains as much as 12 km of Tertiary and Cretaceous sedimentary strata [6], and thus has stimulated the interest of the petroleum industry. Understanding the mass movement processes on the upper slope will be vital to the safe siting of seafloor structures in water depths of > 150 m.

Data Collection

Seismic-reflection profiles and sediment samples (Fig. 1) were collected in 3 successive years of reconnaissance geohazards studies in the Navarin basin area [7, 8]. Seismic systems included 20-80-in^3 airguns, a 500-1000-J minisparker, a hull-mounted Uniboom*, and 3.5 kHz, and 12 kHz sound sources. Sea-floor-sediment samples were collected primarily with a gravity corer (8-cm-diameter barrel); supplementary samples were obtained with box corer and vibra-corer and a Van Veen* grab sampler.

*Any use of trade names in this publication is for descriptive purposes only and does not constitute endoresement by the U.S. Geological Survey.

MORPHOLOGY OF CANYON HEAD

Navarinsky Canyon is the northernmost of the large canyons that dissect the Bering continental margin (Fig. 1). US-USSR 1867 convention line nearly bisects this canyon, which heads in 150 m of water; the canyon extends 270 km across the slope at an average axial gradient of 0.5°, where it debouches onto the continental rise at a depth of ~3,200 m [9]. Navarinsky Canyon is cut into the extremely flat Bering Shelf, which has a gradient of 0.04°-0.1° [9]. The head of the canyon is a broad shallow amphitheater-shaped depression that covers an area of 16,600 km^2. The study area is in the head of the canyon between the two main thalwegs, both of which have axial graidents of ~ 0.2^0 to a depth of 400 m and steepen to ~ 1^0 between 400- and 1,000 m depth [9].

Within the head of Navarinsky Canyon, we mapped a field of large bedforms (1,000- km^2 area) that is bounded by the 200-400-m isobaths and has a sea-floor gradient of 0.6° (Fig. 2). These bedforms have wavelengths of ~ 600 m, heights of 5-15 m, and appear on seismic-reflection records as a stack of climbing dunes that extend to a subbottom depth of 75-100 m (Fig. 3b). Grab samples, box cores, and vibracores collected in the bedform field all recovered moderately well sorted very fine to fine sand. We speculate that the sand in these large bedforms was transported to its present site near the shelf break during Pleistocene low stands of sea level. At that time, the shoreline was near the present 130-140-m isobath and large rivers meandered across the broad flat subaerial reaches of the Bering Shelf [10]. Calculations that take into account the bathymetry, sea-floor gradient, present water depth, sediment type, and oceanographic conditions suggest that these large sand waves are possible products of internal waves [11].

TYPES OF MASS MOVEMENT

Seismic-reflection records from the head of Navarinsky Canyon show two kinds of sea-floor irregularities that we interpret to be the result of mass movement. These phenomena include: (1) depression or pull-apart-like features that adjoin and overlap the field of large bedforms, and (2) a mound or ridge-shaped mass of slide debris. Figures 2 and 3 show the areal relations of all three features -- bedforms, pull-aparts, and slide mass.

Pull-aparts

High-resolution seismic-reflection profiles show unusual breaks in the surface sediment downslope fromt he bedform field (Figs. 2, 3a, 3c). These features are irregularly spaced depressions or notches in the sea floor, ~ 0.1 - 2.0 km apart; they average ~ 50 m wide, have a relief of 3-5 m, and appear to affect only the upper 5-10 m of sediment (Fig. 3c). Absence of side-scan-sonar coverage prevents determination of the true shape of these features, however, the notches are more abundant on lines perpendicular rather than parallel to the isobaths, and thus the notches appear to be oriented parallel to the isobaths. The notches, which are situated between the 350- and 600-m isobaths on a slope of ~ 1^0, have been mapped over an area of 300 km^2 (Fig. 2). The sediment in this part of the canyon is moderately well sorted muddy to fine sand containing some pebbles and granules.

The zone of depressions, notches, or breaks in the surface sediment downslope from th field of large bedforms has the appearance and apparent orientation of pull-aparts or tensional breaks that may result from down slope flow. Another possibility is that these features are shallow craters, pockmarks, or sand boils formed by expulsion of "liquefied" sediment. The

zone of pull-aparts or depressions overlaps the downslope side of the bedform field and thus has developed after the formation of the bedforms and may be continuing to develop at the present time.

Slide Zone

An elongate mound-shaped mass of sediment of hummocky surface morphology that occupies an area of ~ 50 km^2 is situated 4-5 km downslope from the area of surface breaks (Figs. 2, 3a). The hummocky mound of muddy sand has the characteristics commonly associated with a submarine slide mass. This elongate mound is ~ 3 by 14 km, and its long axis is oriented obliquely to the 550 - 800-m isobaths. The mound has a relief of 10-15 m, contains chaotic internal reflectors, affects the upper 30-40 m of sediment, and has formed where the slope gradient of the canyon changes from 1.1° to 2.6° (Fig. 4). Although some seismic-reflection profiles show jumbled and broken reflectors within the mound of sediment, all the profiles show well-developed relatively continuous reflectors beneath the mound starting at a subbottom depth of ~ 40 m (Fig. 4). Both upslope and downslope from the mound the internal reflectors are also continuous at all levels beneath the sea floor.

The hummocky mound of muddy sand that is apparently a product of a shallow slide (Figs. 3a, 4) may have been caused by liquefaction, as postulated for the formation of the pull-aparts, or else these features may have formed totally independently.

TRIGGERING MECHANISM

To generate the types of mass movement that have occurred in the head of Navarinsky Canyon, both a supply of sediment and a mechanism to trigger the mass movement are necessary. The present rate of sediment accumulation on the outer Navarin shelf is relatively low (<20 cm/1,000 yrs on the basis of ^{14}C ages [12]) because of the great distance (>400 km) to the nearest river mouth. The rate of sediment accumulation must have been high during low stands of sea level, however, when large rivers, such as the ancestral Anadyr and Yukon, crossed the subaerially exposed shelf. When the rate of sediment accumulation is rapid, high pore-water pressures can develop and cause sediment instability [13, 14]. Although underconsolidation may be responsible for some of the sediment instability along parts of the Navarin margin, underconsolidation is unlikely in the head of Navarinsky Canyon because the sediment there is primarily noncohesive and pore-water drainage and pressure equalization are presumably rapid.

The Bering Sea is a region of severe storms in which winds commonly exceed 100 km/h (62 mi/h) and, at times, exceed 165 km/h (103 mi/h); waves generated by storms of this magnitude may be as high as 15-20 m [15]. In the head of Navarinsky Canyon, the cohesionless sediment in the area of the pull-aparts and in the slide zone is presently in water depths of 350 m and probably was at >200-m depth during Pleistocene low stands of sea level. On the basis of wave-theory calculations according to the procedures of Seed and Rahman [16], the cohesionless sediment in these areas would not appear to be vulnerable to cyclic loading from large storm waves. Thus, storm waves, either at present or during Pleistocene low stands of sea level, are an unlikely triggering mechanism for the observed failures.

Karl, and others [11] have shown that internal tides and higher frequency internal waves possibly formed the large bedforms in the head of Navarinsky Canyon. Whereas Karl and others [11] determined that energy from 4- and 12-h period internal waves is amplified in the sand-wave field and just downslope from this field, the cohesionless nature of the sediment and the small density contrasts across the pycnocline make internal waves an unlikely triggering mechanism for the mass-movement phenomena farther downslope.

Although the Aleutian island arc is seismically active [17], the great distance (1,000 km) between the Aleutians and Navarinsky Canyon minimizes the effect of horizontal accelerations associated with ground shaking because accelerations drop off rapidly with distance from the epicenter [18]. Even a great ($M>8$) earthquake occurring along the Aleutian Island arc would likely cause low accelerations in Navarinsky Canyon. Additionally, Sereda [19] located the epicenters for two small [$M<4$) earthquakes at Cape Navarin, USSR. Even these events, however, were > 200 km from the head of Navarinsky Canyon and thus would have had little affect on the canyon sediment. Seismicity in the northern Bering Sea has been minimal over the past 85 years. Only eight earthquakes have had epicenters within a radius of 200 km of the study area, all of which were of $M< 5.8$ [17]. On the basis of empirical evidence, for events of this magnitude to cause sediment flow or liquefaction on the Navarinsky slope the epicenter must be within ~ 30 km [20]. Even though we find little evidence in the modern seismological record to support earthquakes as a triggering mechanism, a few traces of shallow faults have been mapped in the head of Navarinsky Canyon [21]. Although none of these faults show offset of the sea floor, they appear to cut sediment as young as Holocene and therefore are considered to be active.

We conclude that earthquakes are the most likely triggering mechanism. In spite of the sparsity of local seismic events in the historical record, we note that our data base covers less than 100 years, and the features under discussion could have formed anytime in the past several thousand years. Thus, the odds of an $M \geq 6.0$ event occurring in the proximity of Navarinsky Canyon and possibly causing liquefaction of the cohesionless sediment are greatly improved.

ACKNOWLEDGEMENTS

We thank Monty Hampton, David Keefer, and Homa Lee for their constructive reviews of the manuscript. This study was supported by the U.S. Geological Survey and the U. S. Bureau of Land Management through interagency agreement with the U. S. National Oceanic and Atmospheric Administration.

REFERENCES

[1] Moore, D. G., 1977. Submarine slides. In B. Voight, (ed.), Rockslides and Avalanches, v. 1, Natural Phenomena. Amsterdam, Elsevier: p. 563-604.

[2] Nardin, T. J., and others, 1979. A review of mass movement processes, sediment and acoustic characteristics, and contrasts in slope and base-of-slope systems versus canyon-fan-basin floor systems. In L. J. Doyle and O. H. Pilkey, (eds.), Geology of Continental Slopes. Society of Economic Paleontologists and Mineralogists Special Publication 27, p. 61-73.

[3] Cook, H. E., Field, M. E., and Gardner, J. V., 1982. Characteristics of sediments on modern and ancient continental slopes. In P. A. Scholle, and D. Spearing, (eds.), Sandstone Depositional evironments: American Association of Petroleum Geologists Memoir 31, p. 329-364.

[4] Scholl, D. W., and others, 1970. The structure and origin of the large submarine canyons of the Bering Sea. Marine Geology, v. 8, p. 187-210.

[5] Carlson, P. R., Karl, H. A., and Quinterno, Paula, 1982. Sedimentologic processes in world's largest submarine canyons, Bering Sea, Alaska. Geological Society of America, Abstracts with Programs, v. 14, p. 459-460.

[6] Marlow, M. S., and others, 1976. Structure and evolution of Bering Sea shelf south of St. Lawrence Island. American Association of Petroleum Geologists Bulletin, v. 60, p. 161-183.

[7] Carlson, P. R., and Karl, H. A., 1981. Seafloor geologic hazards, sedimentology, and bathymetry; Navarin basin province, northern Bering Sea. U.S. Geological Survey Open-File Report 81-1217, 149 p.

[8] Karl, H. A., and Carlson, P. R., 1983. Surface and near-surface geology, Navarin Basin Province: Results of the 1980-81 Field seasons. U.S. Geological Survey Open-File Report 83- , 141 p.

[9] Fischer, J. M., Carlson, P. R., and Karl, H. A., 1982. Bathymetric map of Navarin continental margin, Bering Sea. U.S. Geological Survey Open-File Report 82-1038, 11 p., 1 map sheet.

[10] Karl, H. A., Carlson, P. R., and Lamb, B., 1982. Sediment waves in the head of Navarinsky, Pervenets, and Zhemchug submrine canyons, northwestern Bering Sea. U.S. Geological Survey Circular (Accomplishments in Alaska) 844, p. 141-143.

[11] Karl, H. A., Carlson, P. R., and Lamb, B., 1982. Sediment waves in the head of Navarinsky, Pervenets, and Zhemchug submarine canyons, northwestern Bering Sea. U.S. Geological Survey Circular (Accomplishments in Alaska) 844, p. 141-143.

[12] Carlson, P. R. and Karl, H. A., 1983. Rates of sediment accumulation in Navarin basin province, Bering Sea. In H. A. Karl, and P. R. Carlson, (eds.), Surface and Near-surface Geology, Navarin Basin Province: Results of the 1980-81 Field Seasons. U. S. Geological Survey Open-File Report 83- , in press, 141 p.

[13] Morgenstern, N., 1967. Submarine slumping and the initiation of turbidity currents. In A. F. Richards, (ed.), Marine Geotechnique. Urbanna, Ill., University of Illinois Press, p. 189-220.

[14] Hampton, M. A., and others, 1978. Quantitative study of slope of instability in the Gulf of Alaska. 10th Offshore echnology Conference, Houston, Texas, Proceedings, v. 4, p. 2307-2318.

[15] Brower, W. A., Jr., and others, 1977. Climatic atlas of the outer continental shelf waters and coastal regions of Alaska, v. II, Bering Sea. NOAA OCSEAP Final Report RU 347, Arctic Environmental Information and Data Center, Anchorage, Alaska, Publication B-77, 443 p

[16] Seed, H. B., and Rahman, M. S., 1978. Wave-induced pore pressure in relation to ocean floor stability of cohesionless soils. Marine Geotechnology, v. 3, p. 123-150.

[17] Meyers, H., 1976. A historical summary of earthquake epicenters in and near Alaska. National Oceanographic and Atmospheric Agency Technical Memorandum EDS NGSDC-1, 80 p.

[18] Joyner, W. B., and Boore, D. M., 1981. Peak horizontal acceleration and velocity from strong-motion records from the 1979 Imperial Valley, California, earthquake. Bulletin Seismological Society of America, v. 71, p. 2011-2038.

[19) Sereda, L. I., 1980. Systems of deep-seated faults in the northeast USSR Geotectonics, v. 14, p. 151-160.

[20] Keefer, D. K. 1983. Landslides caused by earthquakes: Bulletin Geological Society of America, in press.

[21) Carlson, P. R., and others, 1982. Geologic hazards in Navarin basin province, northern Bering Sea. 14th Offshore Technology Conference, Houston, Texas, Proceedings, v. 1, p. 73-87.

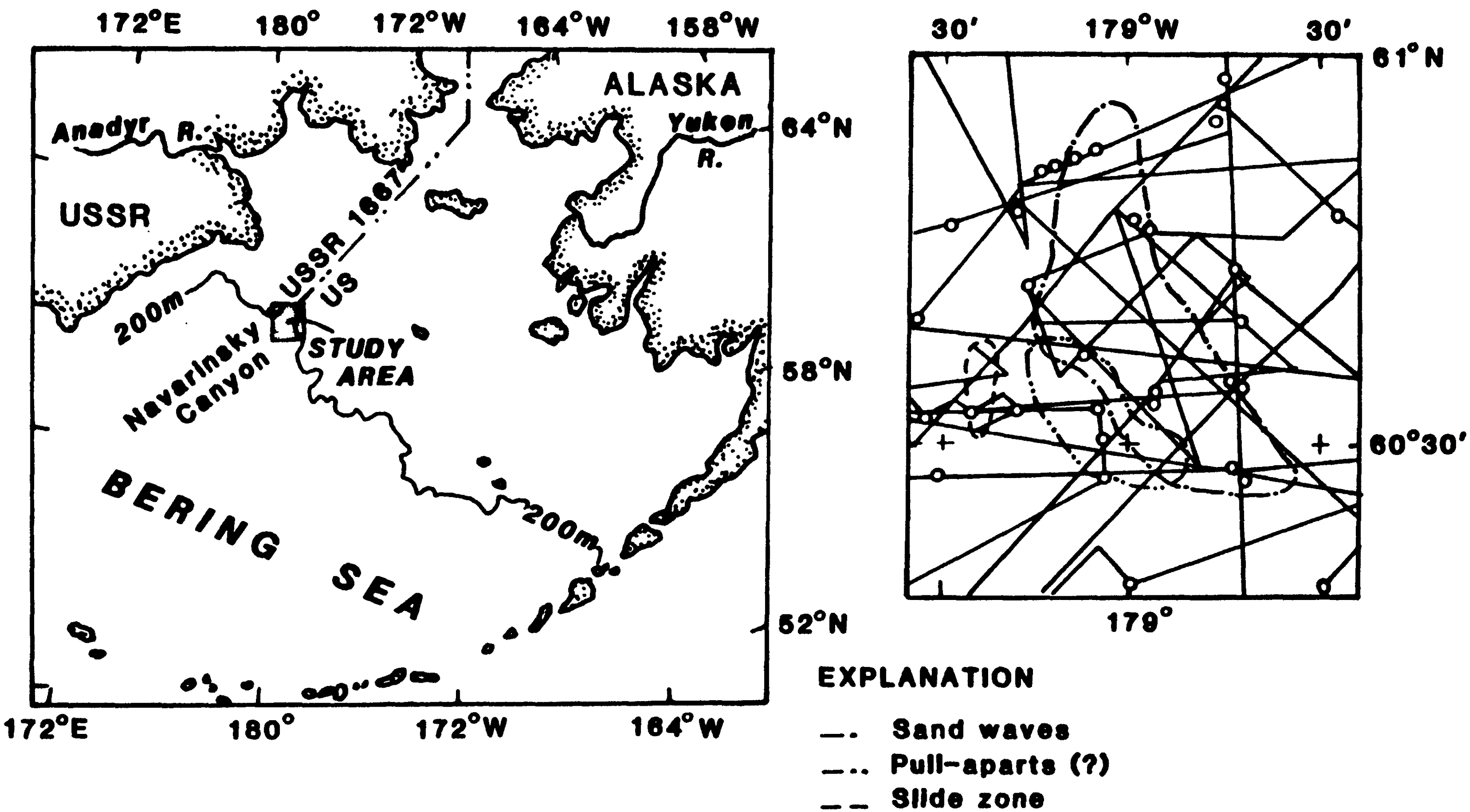

Figure 1. Sketch map of study area in northern Bering Sea, showing locations of high-resolution seismic-reflection lines, sample stations, and areas of sea-floor features.

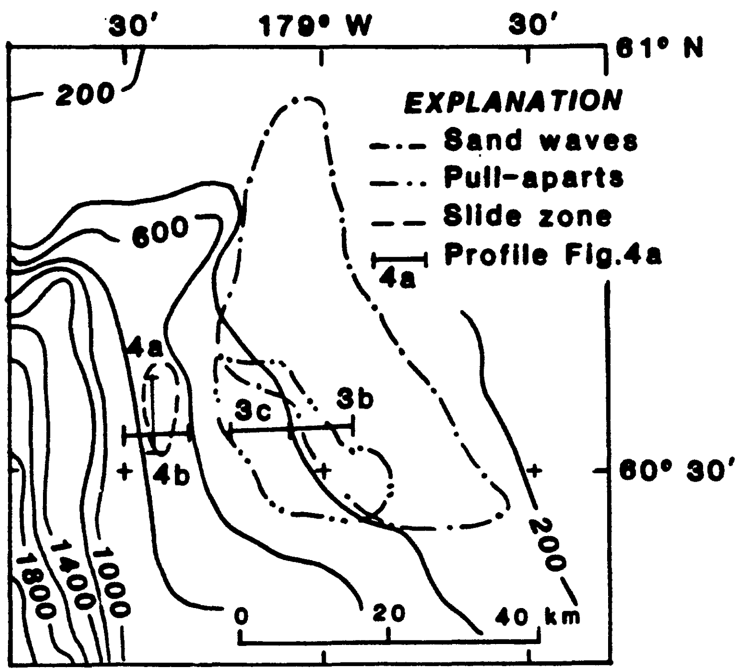

Figure 2. Sea-floor morphologic features in head of Navarinsky Canyon, showing locations of illustrated profiles. Bathymetry after Fischer and others [9]. Contour interval, 200 m.

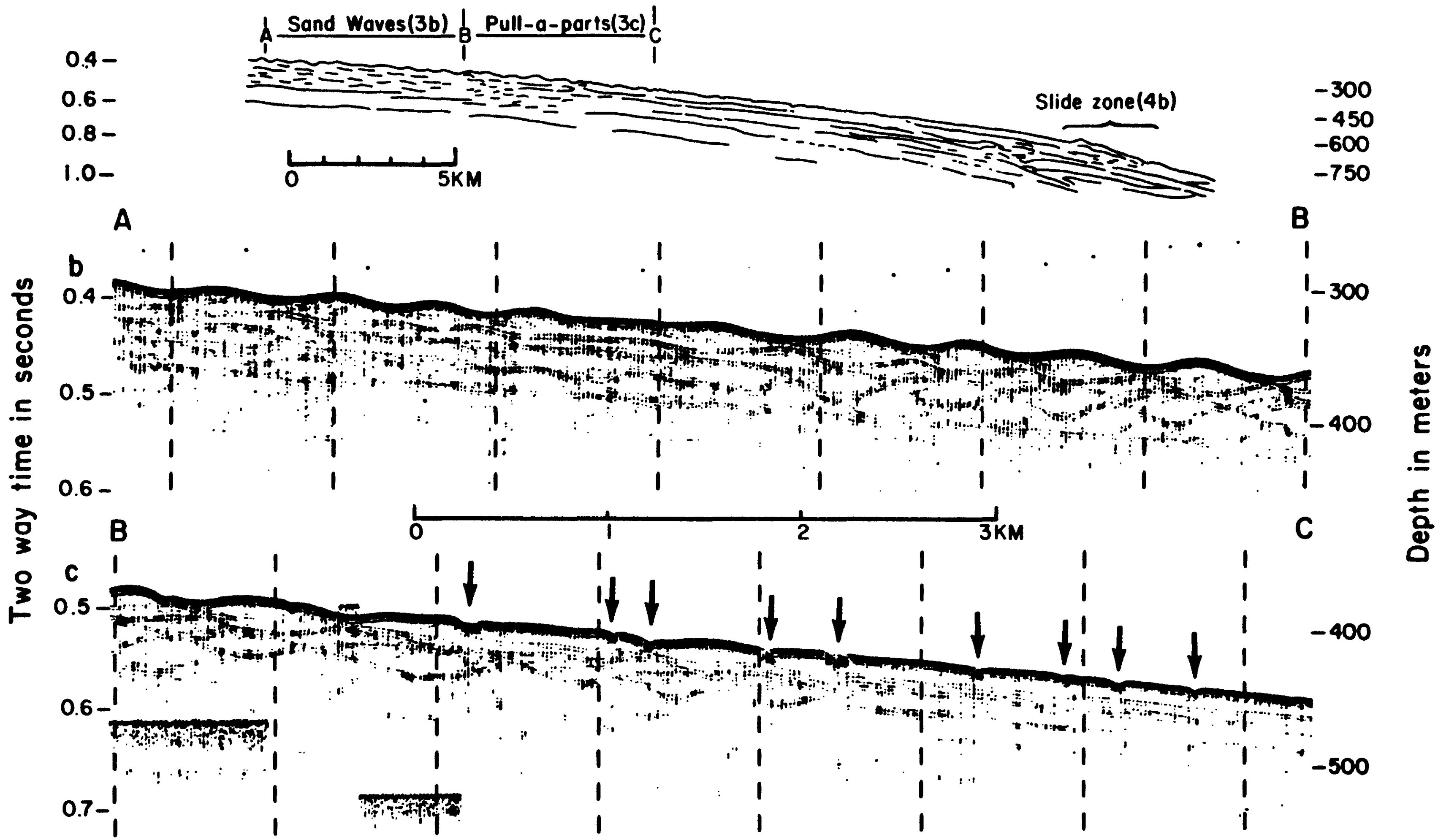

Figure 3. Seismic-reflection profiles in head of Navarinsky Canyon. a, Line drawing of seismic-reflection profiles (20-40-in^3 airguns), showing relative positions of profiles in Figures 3b, 3c, and 4a. b, Minisparker profile (1,000 J), showing sand waves. c, Minisparker profile (1,000 J), showing pull-aparts (arrows). Vertical exaggeration (V.E.) ~7.5x. See Figure 2 for locations.

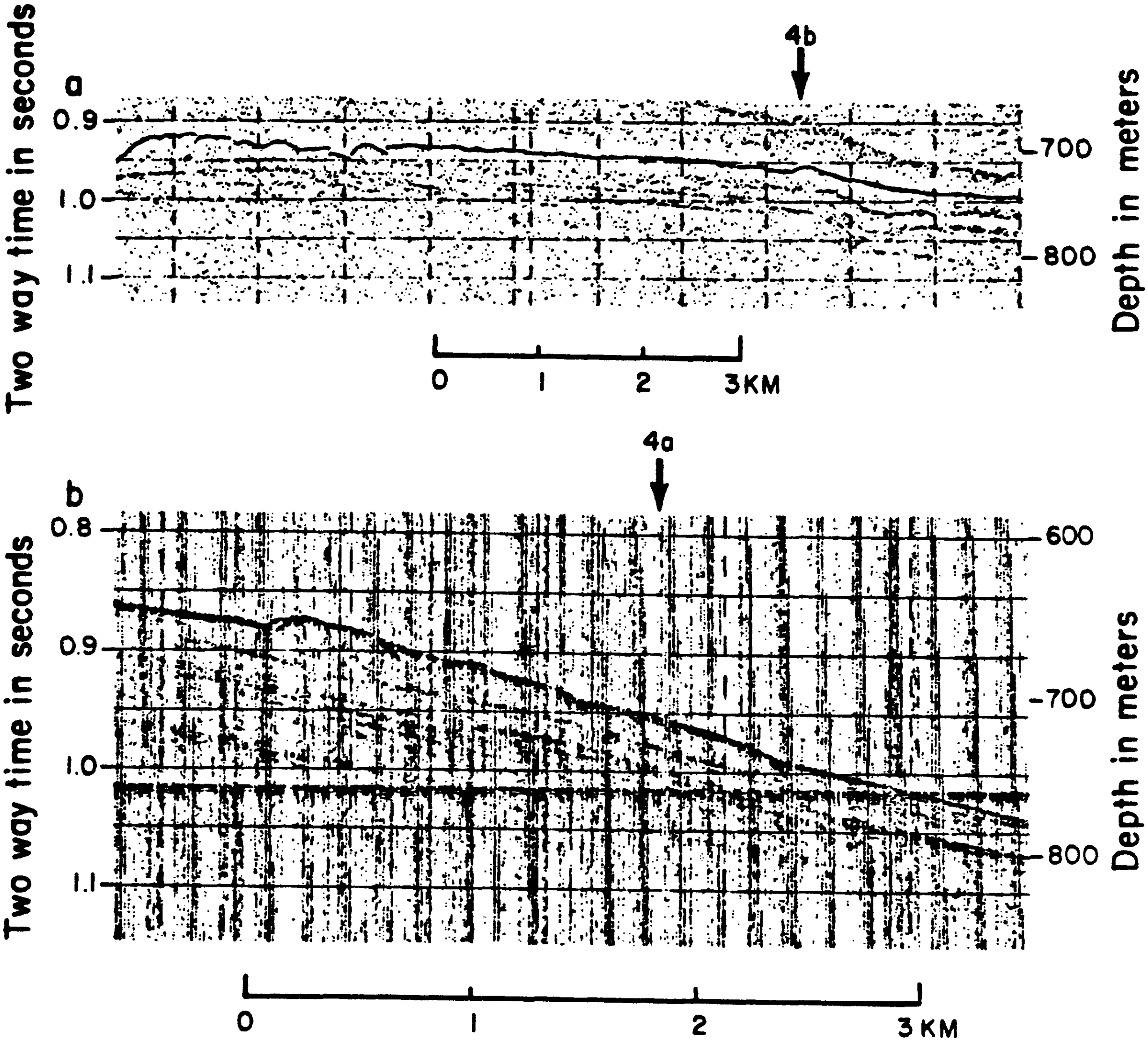

Figure 4. High-resolution profiles, showing slide zone in Navarinsky Canyon. a, 3.5 kHz profile; V.E. ~10x. b, Uniboom profile (1200 J); V.E. ~7.5x. See Figure 2 for locations.